

NEUMANN DOMAINS ON GRAPHS AND MANIFOLDS

LIOR ALON, RAM BAND, MICHAEL BERSUDSKY, SEBASTIAN EGGER

ABSTRACT. The nodal set of a Laplacian eigenfunction forms a partition of the underlying manifold or graph. Another natural partition is based on the gradient vector field of the eigenfunction (on a manifold) or on the extremal points of the eigenfunction (on a graph). The submanifolds (or subgraphs) of this partition are called Neumann domains. This paper reviews the subject, as appears in [2, 6, 7, 46, 62] and points out some open questions and conjectures. The paper concerns both manifolds and metric graphs and the exposition allows for a comparison between the results obtained for each of them.

1. INTRODUCTION

Given a Laplacian eigenfunction on a manifold or a metric graph, there is a natural partition of the manifold or the graph. The partition is dictated by the gradient vector field of the eigenfunction (on a manifold) or by the extremal points of the eigenfunction (on a graph). The submanifolds (or subgraphs) of such a partition are called Neumann domains and the separating lines (or points in the case of a graph) are called Neumann lines (or points). The counterpart of this partition is the nodal partition (with the same terminology of nodal domains, nodal lines and nodal points). This latter partition is extensively studied in the last two decades or so (though interesting results on nodal domains appeared throughout all of the 20-th century and even earlier). When restricting an eigenfunction to a single nodal domain one gets an eigenfunction of that domain with Dirichlet boundary conditions. Similarly, when restricting an eigenfunction to a Neumann domain, one gets a Neumann eigenfunction of that domain (Lemmata 3.1,8.1), which explains the name *Neumann* domain and shows the most basic linkage between nodal domains and Neumann domains.

Neumann domains form a very new topic of study in spectral geometry. They were first mentioned in a paragraph of a manuscript by Zelditch [62]. Shortly afterwards (and independently) a paper by McDonald and Fulling was dedicated to Neumann domains [46]. Since then two additional papers contributed to this topic; one of the authors with Fajman [7] and two of the authors with Taylor [6]. The first part of the current manuscript serves as an exposition of the known results for Neumann domains on two-dimensional manifolds, adding a few supplementary new results and proofs. The second part focuses on Neumann domains on metric graphs and reviews the results which appear in [2]¹. We aim to point out similarities and differences between Neumann domains on manifolds and those on graphs. For this purpose, each of the two parts of the papers is divided to exactly the same subtopics: definitions, topology, geometry, spectral position and count. We also

2000 *Mathematics Subject Classification.* 35Pxx, 57M20, 34B45, 81Q35.

Key words and phrases. Neumann domains, Neumann lines, nodal domains, Laplacian eigenfunctions, Quantum graph, Morse-Smale complexes.

¹While writing this manuscript, we became aware that there is an ongoing research on the related topic of Neumann partitions on graphs. These works in progress are done by Gregory Berkolaiko, James Kennedy, Pavel Kurasov, Corentin Léna and Delio Mugnolo.

include an appendix which contains a short review of relevant results in basic Morse theory, useful for the manifold part of the paper. The summary of the paper provides guidelines for comparison between the manifold results and the graph results. Such a comparison had taught us a great deal in what concerns to the field of nodal domains and yielded a wealth of new results both on manifolds and graphs. As an example we only mention the topic of nodal partitions and refer the interested reader to [5, 13, 15, 16, 17, 20, 24, 36, 38] in order to learn on the evolution of this research direction. In addition to that, we believe that it is beneficial to compare problems between the fields of nodal domains and Neumann domains. We point out such similarities and differences throughout the paper.

Although new in spectral theory, Neumann domains were used in computational geometry, where they are known as Morse-Smale complexes (see the book [64] or [18] for an extensive review). They are used as a tool to analyze sets of measurements on certain spaces and for getting a good qualitative and quantitative acquaintance with the measured functions [23, 27, 28]. Another field of relevance is computer graphics, where Morse-Smale complexes of Laplacian eigenfunctions are applied for surface segmentation [26, 35, 51].

Part 1. Neumann domains on two-dimensional manifolds

2. DEFINITIONS

Let (M, g) be a two-dimensional, connected, orientable and closed Riemannian manifold. We denote by $-\Delta$ the (negative) self-adjoint Laplace-Beltrami operator. Its spectrum is purely discrete since M is compact. We order the eigenvalues $\{\lambda_n\}_{n=0}^\infty$ increasingly, $0 = \lambda_0 < \lambda_1 \leq \lambda_2 \leq \dots$, and denote a corresponding complete system of orthonormal eigenfunctions by $\{f_n\}_{n=0}^\infty$, so that we have

$$(2.1) \quad -\Delta f_n = \lambda_n f_n.$$

We assume in the following that the eigenfunctions f are Morse functions, i.e. have no degenerate critical points². We call such an f a *Morse-eigenfunction*. Eigenfunctions are generically Morse, as shown in [1, 58]. At this point, we refer the interested reader to the appendix, where some basic Morse theory which is relevant to the paper is presented.

In order to define Neumann domains and Neumann lines we introduce the following construction based on the gradient vector field, ∇f . This vector field defines the following flow:

$$(2.2) \quad \begin{aligned} \varphi : \mathbb{R} \times M &\rightarrow M, \\ \partial_t \varphi(t, \mathbf{x}) &= -\nabla f|_{\varphi(t, \mathbf{x})}, \\ \varphi(0, \mathbf{x}) &= \mathbf{x}. \end{aligned}$$

The following notations are used throughout the paper. The set of critical points of f is denoted by $\mathcal{C}(f)$; the sets of saddle points and extrema of f are denoted by $\mathcal{S}(f)$ and $\mathcal{X}(f)$; the sets of minima and maxima of f are denoted by $\mathcal{M}_-(f)$ and $\mathcal{M}_+(f)$, respectively.

For a critical point $\mathbf{x} \in \mathcal{C}(f)$, we define its stable and unstable manifolds by

$$(2.3) \quad \begin{aligned} W^s(\mathbf{x}) &= \{\mathbf{y} \in M \mid \lim_{t \rightarrow \infty} \varphi(t, \mathbf{y}) = \mathbf{x}\} \text{ and} \\ W^u(\mathbf{x}) &= \{\mathbf{y} \in M \mid \lim_{t \rightarrow -\infty} \varphi(t, \mathbf{y}) = \mathbf{x}\}, \end{aligned}$$

²These are critical points where the determinant of the Hessian vanishes.

respectively. Intuitively, these notions may be visualized in terms of surface topography; the stable manifold, $W^s(\mathbf{x})$, may be thought of as a dale (where falling rain droplets would flow and reach \mathbf{x}) and the unstable manifold, $W^u(\mathbf{x})$, as a hill (with opposite meaning in terms of water flow). An interesting scientific account on those appeared by Maxwell already in 1870 [45].

Definition 2.1. [7] Let f be a Morse function.

- (1) Let $\mathbf{p} \in \mathcal{M}_-(f)$, $\mathbf{q} \in \mathcal{M}_+(f)$, such that $W^s(\mathbf{p}) \cap W^u(\mathbf{q}) \neq \emptyset$. Each of the connected components of $W^s(\mathbf{p}) \cap W^u(\mathbf{q})$ is called a *Neumann domain* of f .
- (2) The *Neumann line set* of f is

$$(2.4) \quad \mathcal{N}(f) := \overline{\bigcup_{\mathbf{r} \in \mathcal{S}(f)} W^s(\mathbf{r}) \cup W^u(\mathbf{r})}.$$

Note that the definition above may be applied to any Morse function and not necessarily to eigenfunctions. Indeed, some of the results to follow do not depend on f being an eigenfunction. Yet, the spectral theoretic point of view is the one which motivates us to consider the particular case of Laplacian eigenfunctions.

It is not hard to see from basic Morse theory that Neumann domains are two-dimensional subsets of M , whereas the Neumann line set is a union of one dimensional curves on M (see appendix). Further properties of Neumann domains and Neumann lines are described in the next section.

Figure 2.1 shows an eigenfunction of the flat torus with its partition to Neumann domains.

In the above and throughout the paper, we treat only manifolds without boundary, in order to avoid technicalities and ease the reading. It is possible to define Neumann domains for manifolds with boundary and to prove analogous results for those. The interested reader is referred to [7] for such a treatment.

3. TOPOLOGY OF Ω AND TOPOGRAPHY OF $f|_\Omega$

Let f be an eigenfunction corresponding to an eigenvalue λ and let Ω be a Neumann domain. The boundary, $\partial\Omega$, consists of Neumann lines, which are particular gradient flow lines (see appendix). As the gradient ∇f is tangential to the Neumann lines we get that $\hat{n} \cdot \nabla f|_{\partial\Omega} = 0$, where \hat{n} is normal to $\partial\Omega$. As a consequence we have

Lemma 3.1. $f|_\Omega$ is a Neumann eigenfunction of Ω and corresponds to the eigenvalue λ .

This lemma is the reason for the name *Neumann domains*.

Next, we describe the topological properties of a Neumann domain Ω , as well as the topography of $f|_\Omega$. By topography of a function, we mean the information on its level sets and critical points.

Theorem 3.2. [7, Theorem 1.4]

Let f be a Morse function with a non-empty set of saddle points, $\mathcal{S}(f) \neq \emptyset$.

Let $\mathbf{p} \in \mathcal{M}_-(f)$, $\mathbf{q} \in \mathcal{M}_+(f)$ with $W^s(\mathbf{p}) \cap W^u(\mathbf{q}) \neq \emptyset$.

Let Ω be a connected component of $W^s(\mathbf{p}) \cap W^u(\mathbf{q})$, i.e., Ω is a Neumann domain.

The following properties hold.

- (1) The Neumann domain Ω is a simply connected open set.
- (2) All critical points of f belong to the Neumann line set, i.e., $\mathcal{C}(f) \subset \mathcal{N}(f)$.

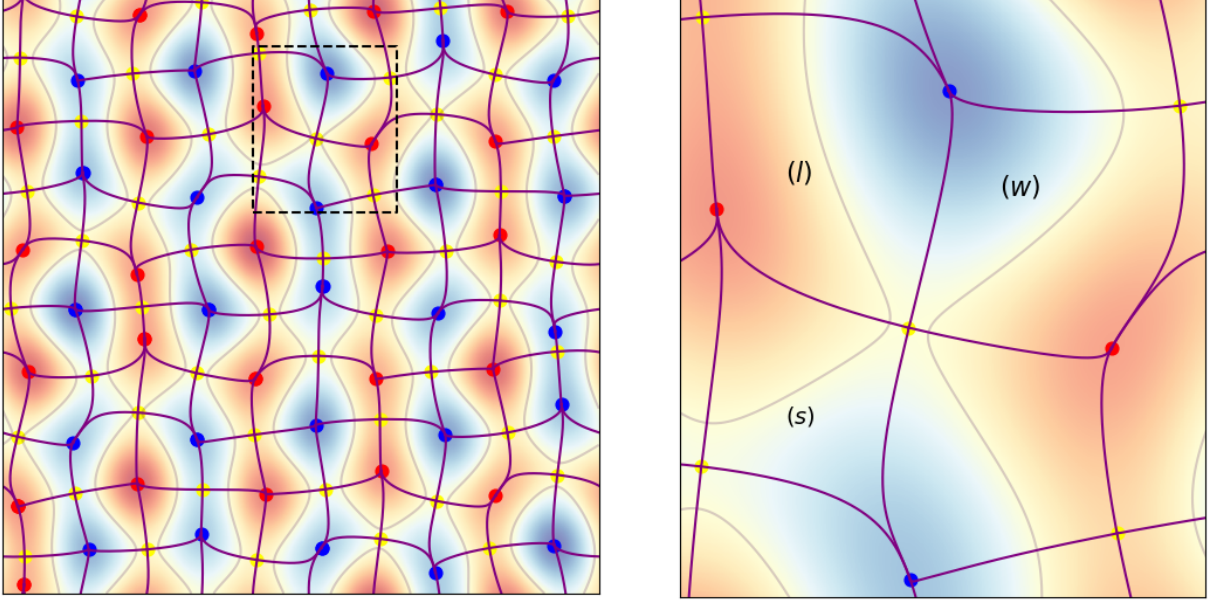


FIGURE 2.1. Left: An eigenfunction corresponding to eigenvalue $\lambda = 25$ of the flat torus whose fundamental domain is $[0, 2\pi] \times [0, 2\pi]$. Red (blue) colors indicate positive (negative) values of the eigenfunction. Red (blue) points mark maximum (minimum) points and yellow points mark saddle points. The nodal set is drawn in grey and the Neumann line set in purple. The Neumann domains are the domains bounded by the Neumann line set. Right: A magnification of the marked square from the left figure. Three Neumann domains are marked by (s), (l) and (w) according to the three distinguished Neumann domain types described in Section 4.1.

- (3) The extremal points which belong to $\overline{\Omega}$ are exactly \mathbf{p}, \mathbf{q} , i.e., $\mathcal{X}(f) \cap \partial\Omega = \{\mathbf{p}, \mathbf{q}\}$.
- (4) If f is a Morse-Smale function³ then $\partial\Omega$ consists of Neumann lines connecting saddle points with \mathbf{p} or \mathbf{q} . In particular, $\partial\Omega$ contains either one or two saddle points (see also Proposition A.7).
- (5) Let $c \in \mathbb{R}$. such that $f(\mathbf{p}) < c < f(\mathbf{q})$. $\overline{\Omega} \cap f^{-1}(c)$ is a smooth, non-self intersecting one-dimensional curve in $\overline{\Omega}$, with boundary points lying on $\partial\Omega$.

This last theorem contains different properties of Neumann domains: claim (1) concerns the topology, claims (2),(3),(4) the critical points, and claim (5) the level sets. A special emphasize should be made for the case when f is a Morse function which is also an eigenfunction. For Laplacian eigenfunctions we have that maxima are positive and minima are negative, i.e., $f(\mathbf{p}) < 0$, $f(\mathbf{q}) > 0$, in the notation of the theorem. Hence we may choose $c = 0$ in claim (5) above and obtain a characterization of the nodal set which is contained within a Neumann domain.

Figure 3.1 shows the two possible schematic shapes of Neumann domains of a Morse-Smale eigenfunction, as implied from the properties above. We complement the figure by noting that there exist Morse functions with Neumann domains of type (ii) but numerical explorations have not revealed any eigenfunction with a Neumann domain of this type.

Let us compare the results above with similar properties of nodal domains. Nodal domains are not necessarily simply connected. On the contrary, it was recently found that

³See appendix for the definition of a Morse-Smale function.

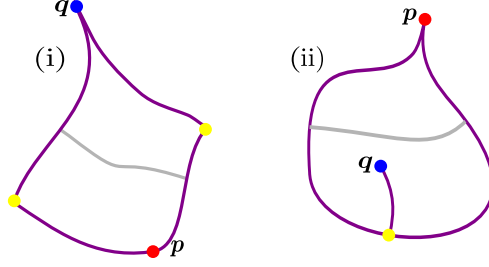


FIGURE 3.1. Two possible types of Neumann domains for a Morse-Smale eigenfunction. Red (blue) discs mark maximum (minimum) points and yellow discs mark saddle points. The nodal set is drawn in grey.

random eigenfunctions may have nodal domains of arbitrarily high genus [52]. Also, there is no upper bound on the number of critical points in a nodal domain. A particular nodal domain may have either minima or maxima (but not both) in its interior and saddle points both in its interior or at its boundary.

4. GEOMETRY OF Ω

4.1. Angles. The angles between Neumann lines meeting at critical points are discussed in [46]. The first two parts of the next proposition summarize the content of theorems 3.1 and 3.2 in [46] and further generalize their result from the Euclidean case to an arbitrary smooth metric. The third part of the proposition is new and concerns the angles between Neumann lines and nodal lines. The proof of the first two parts is almost the same as the one in [46] and we bring it here for completeness.

Proposition 4.1. *Let f be a Morse function on a two dimensional manifold with a smooth Riemannian metric g .*

- (1) *Let \mathbf{c} be a saddle point of f . Then there are exactly four Neumann lines meeting at \mathbf{c} with angles $\pi/2$.*
- (2) *Let \mathbf{c} be an extremal point of f whose Hessian is not proportional to g . Then any two Neumann lines meet at \mathbf{c} with either angle 0 , π , or $\pi/2$.*
- (3) *Further assume that f is a Morse eigenfunction.*
Let \mathbf{c} be an intersection point of a nodal line and a Neumann line of f .
If \mathbf{c} is a saddle point then the angle between those lines is $\pi/4$.
Otherwise, this angle is $\pi/2$.

Proof. We start by some preliminaries that are relevant to proving all parts of the proposition. Let \mathbf{c} be an arbitrary critical point of f . We may find a local coordinate system (x, y) around \mathbf{c} , such that $\mathbf{c} = (0, 0)$ and ∂_x, ∂_y is an orthonormal basis for the tangent space $T_{\mathbf{c}}M$ with respect to the metric g at \mathbf{c} . This means, in particular, that in those coordinates, g at \mathbf{c} is the identity. Thus, we get that the angle between any two vectors, $u, v \in T_{\mathbf{c}}M$ is given by the usual Euclidean inner product, $\langle u, v \rangle_{\mathbb{R}^2}$.

Next, we analyze the Neumann lines which start or end at \mathbf{c} . To do that, we keep in mind that Neumann lines are gradient flow lines which start or end at a saddle point (see appendix), so we first seek for gradient flow lines. Using [10, Lemma 4.4] we deduce that the first (matrix-valued) coefficient in the Taylor expansion of ∇f is $\text{Hess}f|_{\mathbf{c}}$. Hence, the gradient flow equations, (2.2), written in this local coordinate system, satisfy

$$(4.1) \quad \begin{pmatrix} x'(t) \\ y'(t) \end{pmatrix} = -\text{Hess}f|_{\mathbf{c}} \cdot \begin{pmatrix} x(t) \\ y(t) \end{pmatrix} + O(\|(x(t), y(t))\|_{\mathbb{R}^2}^2).$$

As the Hessian is symmetric, we may diagonalize it by an orthonormal change of the coordinates and get

$$\text{Hess}f|_{\mathbf{c}} = \begin{pmatrix} \alpha_x & 0 \\ 0 & \alpha_y \end{pmatrix},$$

where α_x, α_y are both non-zero since f is a Morse function. In those new coordinates, g at \mathbf{c} is still the identity. Hence, the assumption in the second part of the proposition, that the Hessian is not proportional to g , is equivalent to $\alpha_x \neq \alpha_y$. In the vicinity of \mathbf{c} the gradient flow equations, (4.1), may now be approximated by

$$\begin{pmatrix} x'(t) \\ y'(t) \end{pmatrix} = \begin{pmatrix} -\alpha_x x(t) \\ -\alpha_y y(t) \end{pmatrix},$$

where we abuse notation by using (x, y) again to denote the new coordinates which diagonalize the Hessian. The solutions of the above are

$$(4.2) \quad \begin{pmatrix} x(t) \\ y(t) \end{pmatrix} = \begin{pmatrix} a_x e^{-\alpha_x t} \\ a_y e^{-\alpha_y t} \end{pmatrix}, \quad \text{with } a_x, a_y, t \in \mathbb{R}.$$

Consider first the case of $\alpha_x \neq \alpha_y$ both positive, i.e., \mathbf{c} is a minimum point. In this case, all the flow lines (4.2) asymptotically converge to \mathbf{c} as $t \rightarrow \infty$. Recall that $\alpha_x \neq \alpha_y$ by assumption. This allows to assume without loss of generality that $\alpha_y > \alpha_x > 0$. If $a_x \neq 0$, we get that asymptotically as $t \rightarrow \infty$

$$\begin{pmatrix} x(t) \\ y(t) \end{pmatrix} = e^{-\alpha_x t} \begin{pmatrix} a_x \\ a_y e^{-(\alpha_y - \alpha_x)t} \end{pmatrix} \sim e^{-\alpha_x t} \begin{pmatrix} a_x \\ 0 \end{pmatrix}.$$

Any such flow line is tangential to the $\pm \hat{x}$ direction at \mathbf{c} . This gives a continuous family of gradient flow lines, some of which are actually also Neumann lines (this depends on whether or not there is a saddle point at their other end, $t \rightarrow -\infty$). Hence, the possible angles between any of those Neumann lines at \mathbf{c} are either 0 or π . In addition, if $a_x = 0$, we get a gradient flow line which is tangential to the $\pm \hat{y}$ direction at \mathbf{c} . This gradient flow line (which is not necessarily a Neumann line) makes an angle of $\pi/2$ with all others. This proves the second part of the proposition if \mathbf{c} is a minimum point. The case of a maximum is proven in exactly the same manner.

Next we prove the first part of the proposition. If \mathbf{c} is a saddle point, then α_x, α_y are of different signs. The only gradient flow lines, (4.2), which start or end at \mathbf{c} are those for which either $a_x = 0$ or $a_y = 0$. At \mathbf{c} , these lines are either tangential to \hat{x} (if $a_y = 0$) or tangential to \hat{y} (if $a_x = 0$). These are indeed Neumann lines, as they are connected to a saddle point (\mathbf{c}). There are four such Neumann lines, corresponding to all possible sign choices ($a_x = 0$ and a_y is positive\negative or $a_y = 0$ and a_x is positive\negative). The angles between any neighbouring two lines out of the four is therefore $\pi/2$.

Finally, we prove the third part of the proposition. If \mathbf{c} is a critical point, with $\nabla f|_{\mathbf{c}} = 0$, and $f(\mathbf{c}) = 0$ then it must be a saddle point, since maxima of a Laplacian eigenfunction are positive and minima are negative. As f is a Laplace-Beltrami eigenfunction, we get

$$(4.3) \quad 0 = -\lambda f(\mathbf{c}) = \Delta f(\mathbf{c}) = \text{trace} \text{Hess}f|_{\mathbf{c}}.$$

The sum of Hessian eigenvalues is therefore zero and we may denote those by $\pm\alpha$. Choosing a coordinate system which diagonalizes the Hessian at $\mathbf{c} = (0, 0)$, we get

$$f(x, y) = \frac{1}{2} (\alpha x^2 - \alpha y^2) + O(\|(x(t), y(t))\|_{\mathbb{R}^2}^3).$$

This shows that the nodal lines of f at \mathbf{c} may be approximated by $y = \pm x$. We have already seen in the previous part of the proof that the Neumann lines which are connected

to a saddle point, \mathbf{c} , are tangential to either the \hat{x} or the \hat{y} axis and this gives an angle of $\pi/4$ between neighbouring Neumann and nodal lines.

If \mathbf{c} is not a critical point then $\nabla f|_{\mathbf{c}} \neq 0$ and we may write $df(v) = \langle \nabla f|_{\mathbf{c}}, v \rangle_{\mathbb{R}^2}$ for every $v \in T_{\mathbf{c}}M$. By taking v in the direction of the nodal line, we get that the angle between the Neumann line and the nodal line at \mathbf{c} is $\langle \nabla f|_{\mathbf{c}}, v \rangle_{\mathbb{R}^2}$, as g is the identity at \mathbf{c} . Now, since f is constant along the nodal line we have $df(v) = 0$, and get that the angle between the nodal line and the Neumann line is $\pi/2$. \square

Remark. It is also stated in [46, theorem 3.1] that an angle of $\pi/2$ between Neumann lines at an extremal point is non-generic (or “unstable special case”, citing [46]). The proof of the first part of the proposition clarifies why it is so.

The angles between Neumann lines may be observed in Figures 2.1 and 3.1. The exact angles in Figure 2.1 are better seen when zooming in (see right part of the figure).

Proposition 4.1 allows to classify Neumann domains to three distinguished types, as was suggested in [6]. Each Neumann domain has one maxima and one minima on its boundary. Assume that the Neumann domain is of type (i) as depicted in Figure 3.1, i.e., it does not have an extremal point which is connected only to a single Neumann line. We call a Neumann domain

- star-like if both angles at its extremal points are 0,
- lens-like if both angles at its extremal points are π ,
- wedge-like if one of those angles is 0 and the other is π .

Those three types of domains are indicated in Figure 2.1(Right) by (s), (l), (w), correspondingly.

Note that this classification requires a couple of genericity assumptions: that the Hessian at the extremal points is not proportional to the metric and that Neumann lines do not meet perpendicularly at an extremal point (see remark after Proposition 4.1). Indeed, our numeric explorations reveal that Neumann domains are categorized into those three types [6].

4.2. Area to perimeter ratio.

Definition 4.2. [29] Let f be a Morse eigenfunction corresponding to the eigenvalue λ and let Ω be a Neumann domain of f . We define the normalized area to perimeter ratio of Ω by

$$\rho(\Omega) := \frac{|\Omega|}{|\partial\Omega|} \sqrt{\lambda},$$

with $|\Omega|$ being the area of Ω and $|\partial\Omega|$ the total length of its perimeter.

This parameter was introduced in [29] in order to quantify the geometry of nodal domains. A related quantity, $\frac{\sqrt{|\Omega|}}{|\partial\Omega|}$, is a classical one, and it is known to be bounded from above by $\frac{1}{2\sqrt{\pi}}$ (isoperimetric inequality [30]). The value $\frac{|\Omega|}{|\partial\Omega|}$ has also an interesting geometric meaning - it is the mean chord length of the two-dimensional shape Ω . The mean chord length is defined as follows: consider all the parallel chords in a chosen direction and take their average length. The mean chord length is then the uniform average over all directions of that average length⁴.

⁴We thank John Hannay for pointing out this interesting geometrical meaning to us.

There are some numerical explorations, which were performed to study the values of ρ for Neumann domains. In [6] the numerics was done for random eigenfunctions on the flat torus, where the eigenvalues are highly degenerate. More specifically, for a particular eigenvalue, many random eigenfunctions were chosen out of the corresponding eigenspace and the ρ value was numerically computed for all their Neumann domains. The obtained probability distribution of ρ for three different eigenvalues is shown in Figure 4.1,(i). A few interesting observations can be made from those plots. First, it seems that the probability distribution does not depend on the eigenvalue. Furthermore, in Figure 4.1,(ii) the distribution was drawn separately for each of the three types of Neumann domains mentioned in the previous subsection (star, lens and wedge). The lens-like domains tend to get higher ρ values, star-like domains get lower values and the wedge-like are intermediate. Another conclusion which may be drawn from these plots is related to the spectral position of the Neumann domains, which is described in detail in the next section.

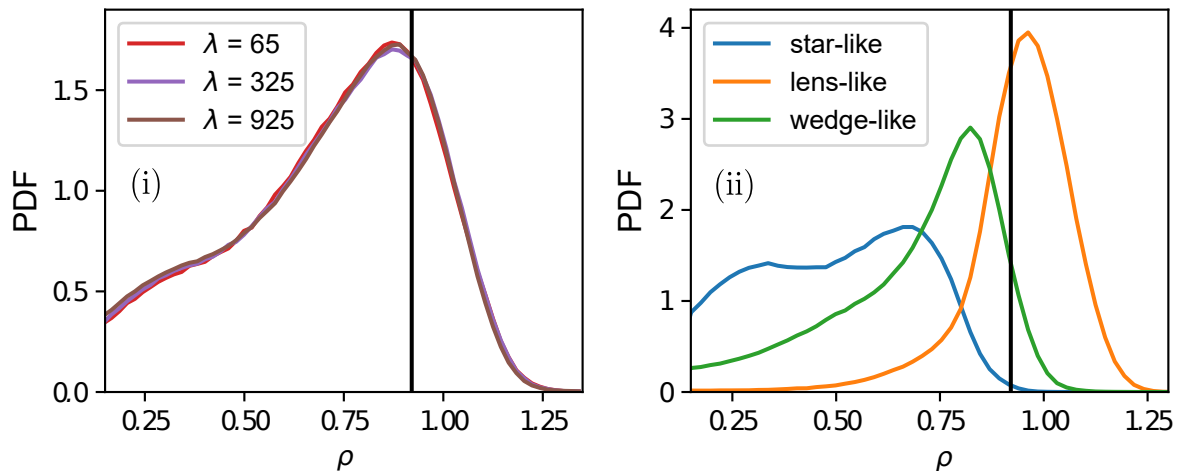


FIGURE 4.1. (i): A probability distribution function of ρ -values of Neumann domains for three different eigenvalues, (ii): A probability distribution function of ρ -values of Neumann domains for $\lambda = 925$ for lens-like, wedge-like and star-like domains. The vertical black line marks the value $\rho \approx 0.9206$ (see Proposition 5.2,(2)). The numerical data was calculated for approximately 9000 eigenfunctions for each eigenvalue. The right plot is based on data of approximately $8.5 \cdot 10^6$ Neumann domains.

We may compare those results with the ones obtained for the distribution of ρ for nodal domains [29]. It is shown in [29] that for nodal domains of separable eigenfunctions $\frac{\pi}{4} < \rho < \frac{\pi}{2}$. Furthermore, it is numerically observed there that these bounds are satisfied with probability 1 for random eigenfunctions. Also, the calculated probability distribution of ρ for nodal domains looks qualitatively different when comparing to Figure 4.1 (see for example figures 1,2,6 in [29]).

5. SPECTRAL POSITION OF Ω

Consider a nodal domain Ξ of some eigenfunction f corresponding to an eigenvalue λ . It is known that $f|_{\Xi}$ is the first eigenfunction (ground-state) of Ξ with Dirichlet boundary

conditions [25]. Equivalently, λ is the lowest eigenvalue in the Dirichlet spectrum of Ξ . This observation is fundamental in many results concerning nodal domains and their counting. In this section we consider the analogous statement for Neumann domains. Our starting point is Lemma 3.1, according to which an eigenvalue λ appears in the Neumann spectrum of each of its Neumann domains. This allows the following definition.

Definition 5.1. Let f be a Morse eigenfunction of an eigenvalue λ and let Ω be a Neumann domain of f . We define the spectral position of Ω as the position of λ in the Neumann spectrum of Ω . It is explicitly given by

$$(5.1) \quad N_\Omega(\lambda) := |\{\lambda_n \in \text{Spec}(\Omega) : \lambda_n < \lambda\}|,$$

where $\text{Spec}(\Omega) := \{\lambda_n\}_{n=0}^\infty$ is the Neumann spectrum of Ω , containing multiple appearances of degenerate eigenvalues and including $\lambda_0 = 0$.

Remark.

- (1) It can be shown (see [6]) that if Ω is a Neumann domain, then its Neumann spectrum is purely discrete. This makes the above well-defined.
- (2) If λ is a degenerate eigenvalue of Ω , then by this definition the spectral position is the lowest position of λ in the spectrum.
- (3) For any Neumann domain, $N_\Omega(\lambda) > 0$. Indeed, $N_\Omega(\lambda) = 0$ is possible only for $\lambda = 0$, but the zero eigenvalue corresponds to the constant eigenfunction and this does not have Neumann domains at all.

A qualitative feeling on the value of $N_\Omega(\lambda)$ might be given by Theorem 3.2. This theorem implies that the topography of $f|_\Omega$ cannot be too complex; its domain, Ω , is simply connected domain; $f|_\Omega$ has no critical points in the interior of Ω ; and its zero set is merely a single simple non-intersecting curve. These observations suggest that $f|_\Omega$ might not lie too high in the spectrum of Ω . Such a belief is also apparent in [62], where it is written that possibly, the spectral position of Neumann domains 'often' equals one, just as in the case of nodal domains. Our task is to study the possible values of $N_\Omega(\lambda)$ for various eigenfunctions and their Neumann domains and to investigate to what extent λ is indeed the first non trivial eigenvalue of Ω ($N_\Omega(\lambda) = 1$). We proceed by relating the spectral position and the area to perimeter ratio (Definition 4.2).

5.1. Connecting spectral position and area to perimeter ratio. The spectral position may be used to bound from above the area to perimeter ratio. This holds as the area to perimeter ratio may be written as

$$\rho(\Omega) = \frac{\sqrt{|\Omega|}}{|\partial\Omega|} \sqrt{|\Omega| \lambda},$$

where the first factor is bounded from above by the classical geometric isoperimetric inequality $\frac{\sqrt{|\Omega|}}{|\partial\Omega|} \leq \frac{1}{2\sqrt{\pi}}$ [30], and the second factor is bounded from above by the spectral isoperimetric inequality, once the spectral position is known. We state below the exact result, whose proof is given in [6].

Proposition 5.2. [6] *Let f be a Morse eigenfunction corresponding to eigenvalue λ . Let Ω be a Neumann domain of f . We have*

- (1) $\rho(\Omega) \leq \sqrt{2}N_\Omega(\lambda)$.
- (2) if $N_\Omega(\lambda) = 1$ then $\rho(\Omega) \leq \frac{i^2}{2} \approx 0.9206$

(3) if $N_\Omega(\lambda) = 2$ then $\rho(\Omega) \leq \frac{j^2}{\sqrt{2}} \approx 1.3019$,

where j denotes the first zero of the derivative of the J_1 Bessel function.

The bounds above may be used to gather information on the spectral position. The calculation of $\rho(\Omega)$ is easier (either numerically or sometimes even analytically) than this of $N_\Omega(\lambda)$. As an example, we bring the probability distribution of ρ given in Figure 4.1,(i). The distribution was calculated numerically for random eigenfunctions on the torus. It is easy to observe that a substantial proportion of the Neumann domains have a ρ value which is larger than 0.9206, the upper bound given in Proposition 5.2(ii). Hence, all those Neumann domains have spectral position which is larger than one, $N_\Omega(\lambda) > 1$. We note that those results seem to be independent of the particular eigenvalue, as the ρ distribution itself seem not to depend on the eigenvalue. Those results are somewhat counter-intuitive, due to what is written above (see discussion after Definition 5.1). Furthermore, when calculating the ρ distribution separately for each of the three different types of Neumann domains (Figure 4.1,(ii)), the higher ρ values of lens-like domains suggest that the spectral position of those domains is higher. These results call for some further investigation of the spectral position dependence on the shape of the Neumann domains.

5.2. Separable eigenfunctions on the torus. The general problem of analytically determining the spectral position is quite involved. Yet, there are some interesting results obtained for separable eigenfunctions on the torus, which we review next. We consider the flat torus with fundamental domain $\mathbb{R}^2/\mathbb{Z}^2$ equipped with the Laplace operator. The eigenvalues are

$$(5.2) \quad \lambda_{a,b} := \frac{\pi^2}{4} \left(\frac{1}{a^2} + \frac{1}{b^2} \right),$$

where

$$(5.3) \quad a := \frac{1}{4m_x}, \quad b := \frac{1}{4m_y}, \quad \text{for } m_x, m_y \in \mathbb{N}.$$

We consider in the following only the separable eigenfunctions, which may be written as

$$(5.4) \quad f_{a,b}(x, y) = \sin\left(\frac{\pi}{2a}x\right) \cos\left(\frac{\pi}{2b}y\right).$$

Half of the Neumann domains of this eigenfunction are star-like and congruent to each other and the other half are lens-like and also congruent (Figure 5.1). We denote those domains by $\Omega_{a,b}^{\text{star}}$ (Figure 5.1(ii)) and $\Omega_{a,b}^{\text{lens}}$ (Figure 5.1(iii)), respectively, and in the following we investigate their spectral position.

First, we may consider only the case $b \leq a$ thanks to the symmetry of the problem. Second, the spectral position of either $\Omega_{a,b}^{\text{star}}$ or $\Omega_{a,b}^{\text{lens}}$ depends only on the ratio $\frac{b}{a}$, as rescaling both a and b by the same factor amounts to an appropriate rescaling of the Neumann domain together with the restriction of the eigenfunction to it. The next theorem summarizes results on the spectral positions of $\Omega_{a,b}^{\text{star}}$ and $\Omega_{a,b}^{\text{lens}}$ from [6] and [7].

Theorem 5.3. [6, 7]

- (1) The set of spectral positions of the **lens**-like domains $\left\{ N_{\Omega_{a,b}^{\text{lens}}}(\lambda_{a,b}) \right\}_{a,b}$ is unbounded. In particular, $N_{\Omega_{a,b}^{\text{lens}}}(\lambda_{a,b}) \rightarrow \infty$ for $\frac{a}{b} \rightarrow \infty$

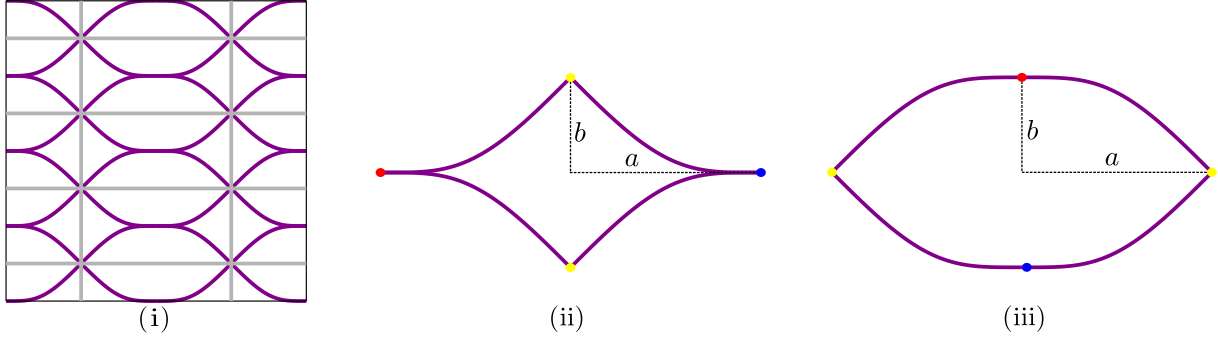


FIGURE 5.1. (i): Grey lines indicate the nodal set and purple lines indicate the Neumann set of a torus eigenfunction $f(x, y) = \sin(2\pi x) \cos(4\pi y)$. (ii) and (iii): the star-like and lens-like Neumann domains of a separable eigenfunction (5.4), with the typical lengths a, b marked as dashed lines. Saddle points are marked by yellow points and extrema by blue and red points.

- (2) There exists $c > 0$ such that if $\frac{a}{b} > c$ then the spectral position of the **star**-like domains is one, i.e., $N_{\Omega_{a,b}^{\text{star}}}(\lambda_{a,b}) = 1$. In addition, $\lambda_{a,b}$ is a simple eigenvalue of $\Omega_{a,b}^{\text{star}}$.

Remark. The condition $\frac{a}{b} > c$ in the second part of the theorem is equivalent to the condition $\frac{m_y}{m_x} > c$ (see (5.3)). As $m_x, m_y \in \mathbb{N}$, this means that the claim in the second part of the theorem is valid for a particular proportion of the separable eigenfunctions on the torus. In particular, combining both parts of the theorem, there is a range of values for a, b for which $N_{\Omega_{a,b}^{\text{star}}}(\lambda_{a,b}) = 1$, but $N_{\Omega_{a,b}^{\text{lens}}}(\lambda_{a,b})$ is as large as we wish.

The proofs of the two parts of this theorem are of different nature. The proof of (1) appears in [7]. It shows by means of contradiction that fixing the value of a and letting b tend to zero the spectral positions $\{N_{\Omega_{a,b}^{\text{lens}}}(\lambda_{a,b})\}_{a,b}$ cannot be bounded. This is done by proving that bounded spectral positions would imply a too rapid growth of the number of Neumann domains. This contradicts the actual growth of the number of Neumann domains, which is explicitly known for those eigenfunctions.

The proof of (2) appears in [6]. It is based on three main ingredients. The first is the symmetry of the domain $\Omega_{a,b}^{\text{star}}$ along a horizontal axis and a vertical axis. The second is a non-standard rearrangement technique using a sector as an intermediate domain [43, 44] and the third is the solution of a suitable geometric isoperimetric problem with a constraint.

The motivation which stands behind Theorem 5.3 is the following. As already mentioned above, it was very natural to believe that generically the spectral position equals one, just as in the case of nodal domains. The first part of the theorem shows that this belief is extremely violated in a particular case. The second part somewhat revives this belief, by showing that this violation which occurs for half of the Neumann domains is somewhat compensated by the other half. We wonder whether this compensation holds for all manifolds. For example, can it be that for any manifold, there exists a constant $0 < p \leq 1$, such that each eigenfunction would have at least a p proportion of its Neumann domains with spectral position equals to one? (see Lemma 6.3, where a similar assumption is employed).

6. NEUMANN DOMAIN COUNT

A wealth of results exists on the number of nodal domains. We start this section by bounding the number of Neumann domains from below in terms of the number of nodal domains. Denote the number of Neumann domains of some eigenfunction f by $\mu(f)$ and the number of its nodal domains by $\nu(f)$. Observe that Theorem 3.2,(5) implies that each Neumann domain intersects with exactly two nodal domains (see discussion following Theorem 3.2). This allows to conclude.

Corollary 6.1. [7]

$$(6.1) \quad \mu(f) \geq \frac{1}{2}\nu(f).$$

Next, we equip the Neumann lines with a graph structure which we call the Neumann set graph. This allows to provide further estimates on the number of the Neumann domains. Let f be a Morse function on a closed two-dimensional manifold and consider its Neumann set graph obtained by taking the vertices (V) to be all critical points, the edges (E) are the Neumann lines connecting critical points and the faces (F) are the Neumann domains. Define the *valency of a critical point*, $\text{val}(\mathbf{x})$, as the number of Neumann lines which are connected to x .

Proposition 6.2. [7] *We have*

$$(6.2) \quad |E| \leq 4|\mathcal{S}(f)|,$$

$$(6.3) \quad \mu(f) \leq 2|\mathcal{S}(f)|,$$

where $\mathcal{S}(f)$ is the set of saddle points of f . If we further assume a Morse-Smale function we get equalities in both (6.2) and (6.3). In addition we have

$$(6.4) \quad \mu(f) = \frac{1}{2} \sum_{\mathbf{x} \in \mathcal{X}(f)} \text{val}(\mathbf{x}) \geq \frac{1}{2}|\mathcal{X}(f)| = \frac{1}{2}(\chi(M) + |\mathcal{S}(f)|),$$

where $\chi(M)$ is the Euler characteristic of the manifold.

The proof of this proposition is done by combining Euler's formula and Morse inequalities for the Neumann set graph.

The ratio $\frac{\mu_n}{n}$. The most fundamental result for the nodal domain count is Courant's bound $\frac{\nu_n}{n} \leq 1$, where ν_n is the nodal count of the n^{th} eigenfunction [25]. Following this, Pleijel had shown that $\limsup_{n \rightarrow \infty} \frac{\nu_n}{n} \leq \left(\frac{2}{j_{0,1}}\right)^2$, where $j_{0,1}$ is the first zero of the J_0 Bessel function, [48]. Many modern works concern the generalizations or improvements of Pleijel's result, as well as the distribution of the ratio $\frac{\nu_n}{n}$ [11, 19, 21, 22, 33, 37, 42, 50, 54]. The study of the distribution of $\frac{\nu_n}{n}$ was initiated in [19]. This distribution was presented there for separable eigenfunctions on the rectangle and the disc. Later, in [33], a more general calculation of the distribution of $\frac{\nu_n}{n}$ was performed. It was done there for the Schrödinger operator on separable systems of any dimension.

In the following, we consider the analogous quantity, $\frac{\mu_n}{n}$, the number of Neumann domains of the n^{th} eigenfunction divided by n . We start by pointing out the connection between $\frac{\mu_n}{n}$, and the spectral position.

Lemma 6.3. *Let (M, g) be a two-dimensional, connected, orientable and closed Riemannian manifold. Assume that there exists $0 < C \leq 1$ such that*

$$(6.5) \quad \sum_{\substack{\Omega \text{ s.t.} \\ N_{\Omega}(\lambda_n)=1}} |\Omega| > C |M|.$$

for all λ_n in the spectrum of M , where the sum above is over all Neumann domains (of an eigenfunction) of λ_n whose spectral position equals one. Then

$$(6.6) \quad \liminf_{n \rightarrow \infty} \frac{\mu_n}{n} \geq C \left(\frac{2}{j} \right)^2.$$

Proof. The Szegő-Weinberger inequality [55, 60] is $\lambda_1(\Omega) |\Omega| \leq \pi j^2$, where j is the first zero of the derivative of the J_1 Bessel function. Consider an eigenfunction f_n of M corresponding to an eigenvalue λ_n . For each Neumann domain Ω of f_n , for which $N_{\Omega}(\lambda_n) = 1$, we have $\lambda_n = \lambda_1(\Omega)$. Combining the Szegő-Weinberger inequality with the assumption in the lemma gives

$$\mu_n \pi j^2 \geq \sum_{\substack{\Omega \text{ s.t.} \\ N_{\Omega}(\lambda_n)=1}} \pi j^2 \geq \sum_{\substack{\Omega \text{ s.t.} \\ N_{\Omega}(\lambda_n)=1}} \lambda_n |\Omega| > C \lambda_n |M|.$$

Applying Weyl asymptotics [61] we get (6.6). \square

Such a result is interesting since it shows that the Neumann count tends to infinity. Similar problems are investigated for the nodal count. It was asked a few years ago by Hoffmann-Ostenhof whether $\limsup_{n \rightarrow \infty} \nu_n = \infty$ holds for any manifold [59]. Following this, Ghosh, Reznikov and Sarnak proved that the number of nodal domains of Maass forms tends to infinity with the eigenvalue [32]. Shortly afterwards, Jung and Zelditch have shown that for negatively curved compact surfaces with some orientation-reversing isometric involution, the number of nodal domains tends to infinity for a density one sub-sequence of the eigenfunctions [40]. Sequentially, they improved upon this result by showing the same asymptotics for non-positively surfaces without the need of an involution [41]. The most recent result is by Zelditch who provided a logarithmic lower bound for the nodal count of eigenfunctions on the first class of manifolds mentioned above [63].

The validity of the inequality (6.6) (and hence the validity of the assumption (6.5)) may be checked by investigating the distribution of $\frac{\mu_n}{n}$, which is our next task.

We consider the separable eigenfunctions of the flat torus \mathbb{T} with fundamental domain $\mathbb{R}^2/\mathbb{Z}^2$. For those eigenfunctions we calculate the limiting probability distribution of $\frac{\mu_n}{n}$.

Given a couple of natural numbers $m_x, m_y \in \mathbb{N}$, we have that

$$(6.7) \quad f_{m_x, m_y}(x, y) = \sin(2\pi m_x x) \cos(2\pi m_y y),$$

is a separable eigenfunction of the following eigenvalue

$$(6.8) \quad \lambda_{m_x, m_y} := 4\pi^2 (m_x^2 + m_y^2),$$

(as in (5.2), (5.4)). Note that the functions $\cos(2\pi m_x x) \cos(2\pi m_y y)$, $\cos(2\pi m_x x) \sin(2\pi m_y y)$, $\sin(2\pi m_x x) \sin(2\pi m_y y)$ together with (6.7) are linearly independent eigenfunctions which belong to the eigenvalue (6.8). The set of all those separable eigenfunctions for all possible values of $m_x, m_y \in \mathbb{N}$ form an orthogonal complete set of eigenfunctions on \mathbb{T} .

We further note that the four eigenfunctions above which correspond to a particular eigenvalue λ_{m_x, m_y} are equal on the torus up to a translation. Hence, all four have the

same number of Neumann domains as f_{m_x, m_y} and we denote this number by μ_{m_x, m_y} . With this we may define the following cumulative distribution function

$$(6.9) \quad F_\lambda(c) := \frac{4}{N_{\mathbb{T}}(\lambda)} \left| \left\{ (m_x, m_y) \in \mathbb{N}^2 : \lambda_{m_x, m_y} < \lambda, \frac{\mu_{m_x, m_y}}{N_{\mathbb{T}}(\lambda_{m_x, m_y})} < c \right\} \right|,$$

where $N_{\mathbb{T}}(\lambda)$ is the spectral position of λ in the torus \mathbb{T} , as in (5.1), and the factor 4 stands for the four eigenfunctions which correspond to λ_{m_x, m_y} . In words, $F_\lambda(c)$ is the proportion of the separable eigenfunctions with eigenvalue less than λ , whose normalized Neumann count is smaller than c . Its limiting distribution is given by the following.

Proposition 6.4. *For $c < \frac{4}{\pi}$*

$$(6.10) \quad \lim_{\lambda \rightarrow \infty} F_\lambda(c) = \frac{1}{2} \int_0^c \frac{1}{\sqrt{1 - (\frac{\pi}{4}x)^2}} dx$$

and for $c \geq \frac{4}{\pi}$

$$\lim_{\lambda \rightarrow \infty} F_\lambda(c) = 1.$$

Proof. The proof consists of a reduction to a lattice counting problem, which allows to derive the limiting distribution. First, observe that the number of Neumann domains of f_{m_x, m_y} is $\mu_{m_x, m_y} = 8m_x m_y$. This holds since f_{m_x, m_y} is Morse-Smale, so that there is an equality in (6.3), and the number of saddle points of f_{m_x, m_y} is the number nodal crossings which is easily shown to be $4m_x m_y$. The symmetry between m_x and m_y in the expression for μ_{m_x, m_y} motivate us to define the set

$$W := \{(m_x, m_y) \in \mathbb{N}^2 : m_x < m_y\},$$

and observe

$$(6.11) \quad \begin{aligned} \forall \lambda \quad & \left| \{(m_x, m_y) \in \mathbb{N}^2 : \lambda_{m_x, m_y} < \lambda\} \right| = 2 \left| \{(m_x, m_y) \in W : \lambda_{m_x, m_y} < \lambda\} \right| \\ & + \left| \{(m_x, m_y) \in \mathbb{N}^2 : m_x = m_y \text{ and } \lambda_{m_x, m_y} < \lambda\} \right| \end{aligned}$$

Plugging (6.11) in (6.9) and taking the limit $\lambda \rightarrow \infty$ gives

$$(6.12) \quad \lim_{\lambda \rightarrow \infty} F_\lambda(c) = \lim_{\lambda \rightarrow \infty} \frac{8}{N_{\mathbb{T}}(\lambda)} \left| \left\{ (m_x, m_y) \in W : \lambda_{m_x, m_y} < \lambda, \frac{\mu_{m_x, m_y}}{N_{\mathbb{T}}(\lambda_{m_x, m_y})} < c \right\} \right|,$$

where we use the Weyl asymptotics, $\lim_{\lambda \rightarrow \infty} N_{\mathbb{T}}(\lambda) = \frac{\lambda}{4\pi}$ [61] and that the second term in the right hand side of (6.11) grows like $\sqrt{\lambda}$ and hence drops when taking the limit.

We analyze (6.12) geometrically. First, $N_{\mathbb{T}}(\lambda)$ counts the number of \mathbb{Z}^2 points with non-zero coordinates, that lie inside a disc of radius $\sqrt{\lambda}$ around the origin. Hence, it may be written as

$$(6.13) \quad N_{\mathbb{T}}(\lambda_{m_x, m_y}) = \pi(m_x^2 + m_y^2) + Err(m_x^2 + m_y^2),$$

where $Err(m_x^2 + m_y^2) = o(m_x^2 + m_y^2)$ [39]. In addition, the point $(m_x, m_y) \in W$ may be characterized by the angle it makes with the x -axis, i.e., $\frac{m_y}{m_x} = \tan \theta_{m_x, m_y}$, so that

$$(6.14) \quad \frac{2m_x m_y}{m_x^2 + m_y^2} = 2 \cos \theta_{m_x, m_y} \cdot \sin \theta_{m_x, m_y} = \sin 2\theta_{m_x, m_y}.$$

With (6.13) and (6.14) we may write

$$\begin{aligned} \frac{\mu_{m_x, m_y}}{N_{\mathbb{T}}(\lambda_{m_x, m_y})} &= \frac{8m_x m_y}{\pi(m_x^2 + m_y^2) (1 + Err(m_x^2 + m_y^2)/\pi(m_x^2 + m_y^2))} \\ &= \frac{1}{(1 + Err(m_x^2 + m_y^2)/\pi(m_x^2 + m_y^2))} \frac{4}{\pi} \cdot \sin 2\theta_{m_x, m_y}. \end{aligned}$$

Let $\varepsilon > 0$. Since $Err(m_x^2 + m_y^2) = o(m_x^2 + m_y^2)$, there exists $\Lambda > 0$ such that for all $(m_x, m_y) \in W$ satisfying $4\pi^2(m_x^2 + m_y^2) > \Lambda$, the following holds

$$(6.15) \quad \frac{1}{1 + \varepsilon} \frac{4}{\pi} \sin 2\theta_{m_x, m_y} < \frac{\mu_{m_x, m_y}}{N_{\mathbb{T}}(\lambda_{m_x, m_y})} < \frac{1}{1 - \varepsilon} \frac{4}{\pi} \sin 2\theta_{m_x, m_y}.$$

The limiting cumulative distribution (6.12) may be slightly rewritten as

$$\lim_{\lambda \rightarrow \infty} F_{\lambda}(c) = \lim_{\lambda \rightarrow \infty} \frac{8}{N_{\mathbb{T}}(\lambda)} \left| \left\{ (m_x, m_y) \in W : \Lambda < \lambda_{m_x, m_y} < \lambda, \frac{\mu_{m_x, m_y}}{N_{\mathbb{T}}(\lambda_{m_x, m_y})} < c \right\} \right|,$$

where the additional condition $\Lambda < \lambda_{m_x, m_y}$ removes only a finite number of points from the set and does not affect the limit. We may now use (6.15) to get the following inequalities by set inclusion

$$(6.16)$$

$$\begin{aligned} \lim_{\lambda \rightarrow \infty} F_{\lambda}(c) &\leq \\ \lim_{\lambda \rightarrow \infty} \frac{8}{N_{\mathbb{T}}(\lambda)} &\left| \left\{ (m_x, m_y) \in W : \Lambda < \lambda_{m_x, m_y} < \lambda \text{ and } \theta_{m_x, m_y} < \frac{1}{2} \arcsin \left(\frac{\pi c(1 + \varepsilon)}{4} \right) \right\} \right|, \end{aligned}$$

and

$$(6.17)$$

$$\begin{aligned} \lim_{\lambda \rightarrow \infty} F_{\lambda}(c) &\geq \\ \lim_{\lambda \rightarrow \infty} \frac{8}{N_{\mathbb{T}}(\lambda)} &\left| \left\{ (m_x, m_y) \in W : \Lambda < \lambda_{m_x, m_y} < \lambda \text{ and } \theta_{m_x, m_y} < \frac{1}{2} \arcsin \left(\frac{\pi c(1 - \varepsilon)}{4} \right) \right\} \right|, \end{aligned}$$

where in the above we assume that $0 \leq c < \frac{4}{\pi}$ and ε is small enough so that $\pi c(1 + \varepsilon)/4 \leq 1$, and in particular $\arcsin(\pi c(1 + \varepsilon)/4)$ is well defined.

We notice that the right hand sides of (6.16) and (6.17) correspond to counting integer lattice points which are contained within a certain sector. This number of points grows like the area of the corresponding sector [39], i.e.,

$$\begin{aligned} &\left| \left\{ (m_x, m_y) \in W : \Lambda < \lambda_{m_x, m_y} < \lambda, \theta_{m_x, m_y} < \frac{1}{2} \arcsin \left(\frac{\pi c(1 \pm \varepsilon)}{4} \right) \right\} \right| = \\ (6.18) \quad &\underbrace{\frac{1}{4} \arcsin \left(\frac{\pi c(1 \pm \varepsilon)}{4} \right) \frac{\lambda - \Lambda}{4\pi^2}}_{\text{area of a sector}} + o(\lambda). \end{aligned}$$

Plugging (6.18) in the bounds (6.16), (6.17) and using (6.13) gives

$$\frac{2}{\pi} \arcsin \left(\frac{\pi c(1 - \varepsilon)}{4} \right) \leq \lim_{\lambda \rightarrow \infty} F_{\lambda}(c) \leq \frac{2}{\pi} \arcsin \left(\frac{\pi c(1 + \varepsilon)}{4} \right).$$

As $\varepsilon > 0$ is arbitrary we get

$$\begin{aligned} \forall c < \frac{4}{\pi} \quad \lim_{\lambda \rightarrow \infty} F_\lambda(c) &= \frac{2}{\pi} \arcsin\left(\frac{\pi c}{4}\right), \\ &= \frac{1}{2} \int_0^c \frac{1}{\sqrt{1 - (\frac{\pi}{4}x)^2}} dx, \end{aligned}$$

which proves (6.10). Finally note that we have $\lim_{c \rightarrow \frac{4}{\pi}} \lim_{\lambda \rightarrow \infty} F_\lambda(c) = 1$, and as $F_\lambda(c)$ is a cumulative distribution function we get $\lim_{\lambda \rightarrow \infty} F_\lambda(c) = 1$ for $c \geq \frac{4}{\pi}$. \square

Remark. The calculation in the proof above may be considered as a particular case of those done in [33]. The proof here is explicitly tailored for the purpose of the current paper.

The next figure shows the probability distribution given in (6.10) and compares it to a numerical examination of the probability distribution of $\frac{\mu_n}{n}$ for the separable eigenfunctions on the torus.

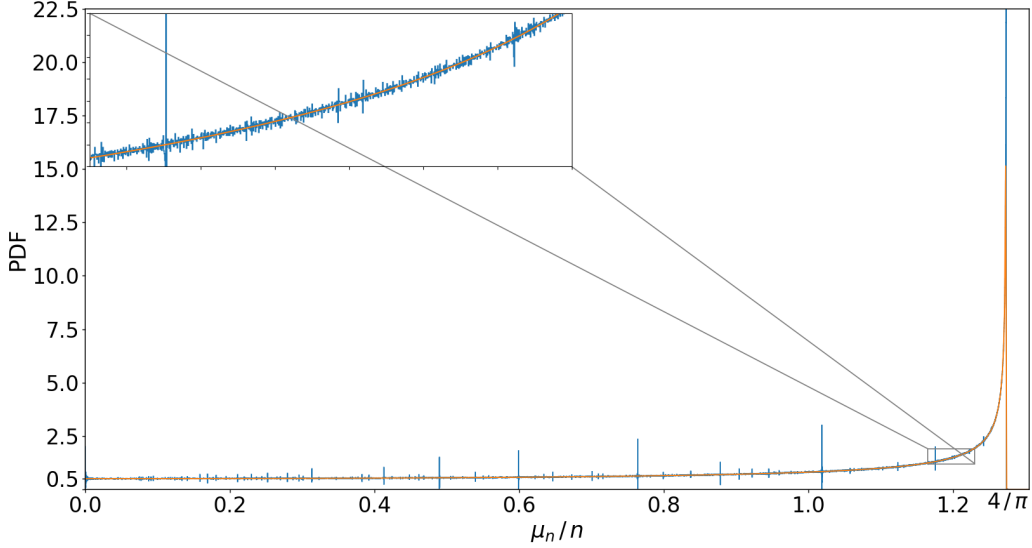


FIGURE 6.1. *Orange curve:* the probability distribution of $\frac{\mu_n}{n}$ as given in (6.10). *Blue curve:* a numerical calculation of this distribution as calculated for the first $2 \cdot 10^8$ torus eigenfunctions.

Examining the $\frac{\mu_n}{n}$ distribution leads to the following. First, we note that $\frac{\mu_n}{n}$ may get arbitrarily low values for a positive proportion of the eigenfunctions. This is in contradiction with (6.6) and therefore we conclude that the separable eigenfunctions on the flat torus do not satisfy assumption (6.5) in Lemma 6.3. Indeed, it can be checked directly in this case that the total area of all star domains goes to zero as the eigenvalue $\lambda_{a,b}$ tends to infinity. Therefore their total area does not satisfy (6.5).

Turning our attention to the higher values of $\frac{\mu_n}{n}$ we notice that $\frac{\mu_n}{n} > 1$ for a positive proportion of the eigenfunction. This means that the strict Courant bound does not apply to the Neumann domain count. Yet, we ask whether an upper bound of the form $\mu_n \leq h(n)$ exists, with h being possibly a linear function. If so, a possible upper bound might be suggested by the separable eigenfunctions, for which $h(n) = \frac{4}{\pi}n$, serves as a

bound. Furthermore, the Courant-like bound on the Neumann count for metric graphs (11.2), to be discussed in the next part, is a suggestive evidence for the existence of a Courant-like bound in the case of manifolds⁵.

Part 2. Neumann domains on metric graphs

7. DEFINITIONS

7.1. Discrete graphs and graph topologies. We denote by $\Gamma = (\mathcal{V}, \mathcal{E})$ a connected graph with finite sets of vertices \mathcal{V} and edges \mathcal{E} . We allow the graph edges to connect either two distinct vertices or a vertex to itself. In the latter case, such an edge is called a loop.

For a vertex $v \in \mathcal{V}$, its *degree*, d_v , equals the number of edges connected to it. The set of graph vertices of degree one turns out to be useful and we denote it by

$$\partial\Gamma := \{v \in \mathcal{V} : d_v = 1\}.$$

We call the vertices in $\partial\Gamma$, *boundary vertices* and the rest of the vertices, $\mathcal{V} \setminus \partial\Gamma$, are called *interior vertices*.

An important topological quantity of graphs is the first Betti number (dimension of the first homology group) given, for a connected graph, by

$$(7.1) \quad \beta := |\mathcal{E}| - |\mathcal{V}| + 1.$$

The value of β is the number cycles needed to span the space of cycles on the graph. By definition a graph is simply connected when $\beta = 0$, and such a graph is called a tree graph. Two particular examples of trees are star graphs and path graphs. A star graph is a graph with one interior vertex which is connected by edges to the other $|\mathcal{V}| - 1$ boundary vertices. A path graph is a connected graph with two boundary vertices and $|\mathcal{V}| - 2$ interior vertices which are all of degree two. The path graph which shows up later in this paper is the simplest graph of only two vertices connected by a single edge.

7.2. Spectral theory of metric graphs. A *metric graph* is a discrete graph for which each edge, $e \in \mathcal{E}$, is identified with a one-dimensional interval $[0, L_e]$ of a positive finite length L_e . We assign to each edge $e \in \mathcal{E}$ a coordinate, x_e , which measures the distance along the edge from one of the two boundary vertices of e .

A function on the graph is described by its restrictions to the edges, $\{f|_e\}_{e \in \mathcal{E}}$, where $f|_e : [0, L_e] \rightarrow \mathbb{C}$. We equip the metric graphs with a self-adjoint differential operator,

$$(7.2) \quad -\Delta : f|_e(x_e) \mapsto -\frac{d^2}{dx_e^2} f|_e(x_e),$$

⁵While writing this manuscript we became aware of a work in progress by Buhovski, Logunov, Nazarov and M. Sodin, which might disprove the existence of such a bound.

which is the Laplacian⁶. It is most common to call this setting of a metric graph and an operator by the name quantum graph.

To complete the definition of the operator we need to specify its domain. We consider functions which belong to the following direct sum of Sobolev spaces

$$(7.3) \quad H^2(\Gamma) := \bigoplus_{e \in \mathcal{E}} H^2([0, L_e]) .$$

In addition we require some matching conditions on the graph vertices. A function $f \in H^2(\Gamma)$ is said to satisfy the Neumann vertex conditions at a vertex v if

(1) f is continuous at $v \in \mathcal{V}$, i.e.,

$$(7.4) \quad \forall e_1, e_2 \in \mathcal{E}_v \quad f|_{e_1}(0) = f|_{e_2}(0),$$

where \mathcal{E}_v is the set of edges connected to v , and for all $e \in \mathcal{E}_v$, $x_e = 0$ at v .

(2) The outgoing derivatives of f at v satisfy

$$(7.5) \quad \sum_{e \in \mathcal{E}_v} \left. \frac{df}{dx_e} \right|_e (0) = 0.$$

Requiring these conditions at each vertex leads to the operator (7.2) being self-adjoint and its spectrum being real and bounded from below [14]. In addition, since we only consider compact graphs, the spectrum is discrete. We number the eigenvalues in the ascending order and denote them by $\{\lambda_n\}_{n=0}^\infty$ and their corresponding eigenfunctions by $\{f_n\}_{n=0}^\infty$. As the operator is both real and self-adjoint, we may choose the eigenfunctions to be real, which we will always do.

In this paper, we only consider graphs whose vertex conditions are Neumann at all vertices, and call those *standard graphs*. A special attention should be given to vertices of degree two. Introducing such a vertex at the interior of an existing edge (thus splitting this edge into two) and requiring Neumann conditions at this vertex does not change the eigenvalues and eigenfunctions of the graph. The same holds when removing a degree two vertex and uniting two existing edges into one. This spectral invariance allows us to assume in the following that standard graphs do not have any vertices of degree two. Furthermore, the only graph, all of whose vertices are of degree two (or equivalently has no vertices at all) is the single loop graph. We assume throughout the paper that our graphs are different than the single loop graph and call those *nontrivial graphs*.

The spectrum of a standard graph is non-negative, which means that we may represent the spectrum by the non-negative square roots of the eigenvalues, $k_n = \sqrt{\lambda_n}$. For convenience we abuse terminology and call also $\{k_n\}_{n=0}^\infty$ the eigenvalues of the graph. Most of the results and proofs in this part are expressed in terms of those eigenvalues. A Neumann graph has $k_0 = 0$ with multiplicity which equals the number of graph components. The common convention is that if an eigenvalue is degenerate (i.e. non simple) it appears more than once in the sequence $\{k_n\}_{n=0}^\infty$. For any such degenerate eigenvalue, we pick a basis for its eigenspace and all members of this basis appear in the sequence $\{f_n\}_{n=0}^\infty$. Obviously, this makes the choice of the sequence $\{f_n\}_{n=0}^\infty$ non unique. It is important to note that all the statements to follow hold for any choice of $\{f_n\}_{n=0}^\infty$.

⁶More general operators appear in the literature. See for example [14, 34].

7.3. Neumann points and Neumann domains. For metric graphs, the nodal point set of a function is the set of points at which the function vanishes. Removing the nodal point set from the graph, splits it into connected components and those are called nodal domains. The Neumann set and Neumann domains are similarly defined, but before doing so we need to restrict to particular classes of functions.

Definition 7.1. Let Γ be a nontrivial standard graph and f be an eigenfunction of Γ .

- (1) We call f a *Morse eigenfunction* if for each edge e , $f|_e$ is a Morse function. Namely, at no point in the interior of e both the first and the second derivatives of f vanish.
- (2) We call an eigenfunction f *generic* if it is a Morse eigenfunction and in addition satisfies all of the following:
 - (a) f corresponds to a simple eigenvalue.
 - (b) f does not vanish at any vertex.
 - (c) f has no extremal points at interior vertices.

An equivalent characterization of a Morse eigenfunction is

Lemma 7.2. *Let f be a non-constant eigenfunction. f is Morse if and only if there exists no edge e such that $f|_e \equiv 0$.*

Proof. First, observe that a non-constant eigenfunction of the Laplacian vanishes at an interior point of an edge if and only if the second derivative vanishes at that point. Therefore, if f is a Morse eigenfunction then there is no interior point at which both the function and its derivative vanish. This means that a Morse eigenfunction cannot vanish entirely at a graph edge. As for the converse, if f is a non-Morse eigenfunction then there exists \mathbf{x} , an interior point of an edge e , such that $f|_e'(\mathbf{x}) = f|_e''(\mathbf{x}) = 0$. By the same argument as above, this means that either $f|_e(\mathbf{x}) = 0$ or $f|_e$ is the constant eigenfunction. The vanishing of $f|_e$ and its first derivative at the same point, together with $f|_e$ being a solution of an ordinary differential equation of second order implies $f|_e \equiv 0$. \square

We complement this lemma and note that the constant eigenfunction, corresponding to $k_0 = 0$ is not a Morse function. This, together with the lemma, implies that a Morse eigenfunction may vanish only at isolated points of the graph; the same holds for its derivative. This quality allows the following.

Definition 7.3. Let f be a Morse eigenfunction.

- (1) A Neumann point of f is an extremal point (maximum or minimum) not located at a boundary vertex. Namely, the set of Neumann points is

$$(7.6) \quad \mathcal{N}(f) := \{\mathbf{x} \in \Gamma \setminus \partial\Gamma : \mathbf{x} \text{ is an extremal point of } f\}.$$

Note that we reuse here the notation for the Neumann lines in the manifold case, (2.4).

- (2) A Neumann domain of f is a closure of a connected component of $\Gamma \setminus \mathcal{N}(f)$. The closure is done by adding vertices of degree one at the open endpoints of the connected component.

Figure 7.1 shows the Neumann point and Neumann domains of a particular eigenfunction.

Remark.

- (1) The definition implies that a Neumann point is either a point $\mathbf{x} \in \Gamma \setminus \mathcal{V}$ at some interior of an edge such that $f'(\mathbf{x}) = 0$, or it is a vertex $v \in \mathcal{V}$ such that all outgoing

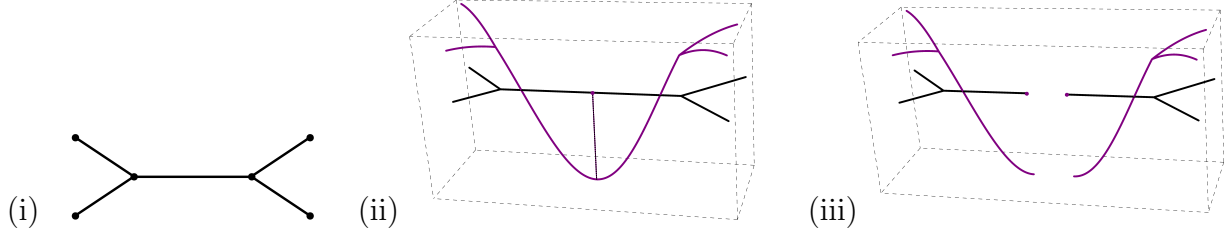


FIGURE 7.1. (i) A graph Γ (ii) An eigenfunction f of Γ , with its single Neumann point marked (iii) A decomposition of Γ into the Neumann domains of f .

derivatives of f at that vertex vanish. The latter possibility does not occur if f is generic.

- (2) From the proof of Lemma 7.2 we learn that no point can be both a nodal point and a Neumann point.

All the results to follow concerning Neumann points and Neumann domains are stated for either Morse or generic eigenfunctions. We start by stating what proportion of the eigenfunctions are Morse and which proportion of the Morse ones are generic. In order to do so, we need to assume that the set of edge lengths is linearly independent over the field \mathbb{Q} . We call such lengths *rationally independent* and we will assume this for the graph edge lengths in some of the propositions to follow.

Proposition 7.4. [2, 3] *Let Γ be a nontrivial standard graph, with rationally independent edge lengths $\{L_e\}_{e \in \mathcal{E}}$. Let $\{f_n\}_{n=0}^\infty$ be a complete set of eigenfunctions of Γ .*

- (1) *The proportion of Morse eigenfunctions is given by*

$$(7.7) \quad d_L := \lim_{N \rightarrow \infty} \frac{|\{n \leq N : f_n \text{ is Morse}\}|}{N} = 1 - \frac{1}{2} \frac{\sum_{e \in \mathcal{E}_L} L_e}{\sum_{e \in \mathcal{E}} L_e},$$

where \mathcal{E} is the set of graph edges and \mathcal{E}_L is a subset of \mathcal{E} consisting of all edges which form loops (edges which connect a vertex to itself).

- (2) *The proportion of generic eigenfunctions out of the Morse ones is*

$$(7.8) \quad \lim_{N \rightarrow \infty} \frac{|\{n \leq N : f_n \text{ is generic}\}|}{|\{n \leq N : f_n \text{ is Morse}\}|} = \frac{1}{d_L} \lim_{N \rightarrow \infty} \frac{|\{n \leq N : f_n \text{ is generic}\}|}{N} = 1.$$

Namely, almost all Morse eigenfunctions are generic.

Remark.

- (1) The limits in (7.7) and (7.8) exist even without assuming that the edge lengths are rationally independent. This assumption is needed to obtain the exact values of those limits.
- (2) From the proposition we get that at least half of the eigenfunctions are Morse, and if a graph has no loops, almost all eigenfunctions are Morse and generic.
- (3) The proof of (7.7) is similar to the proof of proposition A.1 in [3]. The proof of (7.8) appears in [2].

8. TOPOLOGY OF Ω AND TOPOGRAPHY OF $f|_\Omega$

Let Γ be a nontrivial standard graph and f an eigenfunction of Γ corresponding to the eigenvalue k . Formally, every Neumann domain Ω of f may be considered as a subgraph of Γ , if we add degree two vertices to Γ at all the Neumann points of f (see discussion

on those vertices in Section 7.2). In particular, a Neumann domain is a closed set (by Definition 7.3). This difference from the manifold case (where Neumann domains are open sets) is technical and serves our need to consider Ω as a metric graph on its own. Being a metric graph, we take the usual Laplacian on Ω and impose Neumann vertex conditions at all of its vertices, so that Ω is considered as a standard graph. Note that the restriction of $f|_{\Omega}$ to the edges of Ω trivially satisfies $f'' = -k^2 f$. It also obeys Neumann vertex conditions at all vertices of Ω , as each vertex is either a vertex of Γ or a point $\mathbf{x} \in \Gamma$ in an interior of an edge for which $f'(\mathbf{x}) = 0$. This gives the following, which is analogous to Lemma 3.1.

Lemma 8.1. *$f|_{\Omega}$ is an eigenfunction of the standard graph Ω and corresponds to the eigenvalue k .*

Remark. Furthermore, it can be proved that if f is a generic eigenfunction and Ω is a tree graph then $f|_{\Omega}$ is also generic [2].

8.1. Possible topologies for Neumann domains. In this subsection we discuss which graphs may be obtained as a Neumann domain. The next lemma shows that if we consider an eigenfunction, f , whose eigenvalue is high enough, each of its Neumann domains is either a path graph or a star graph. A star Neumann domain contains an interior vertex of the graph, and a path Neumann domain is contained in a single edge of the graph (see Figure 8.1).

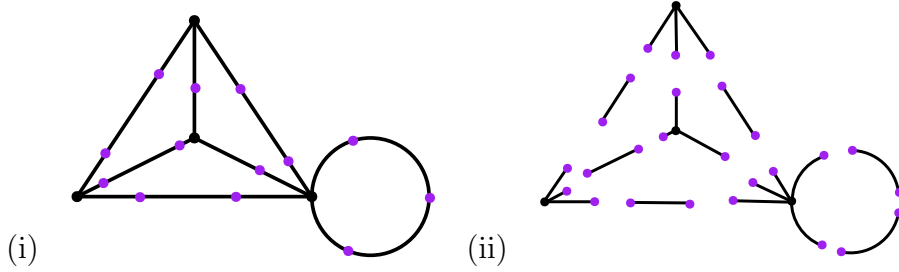


FIGURE 8.1. (i) A graph Γ with Neumann points (in purple) of a given eigenfunction (ii) The decomposition of the graph to the corresponding Neumann domains.

Lemma 8.2. *Let Γ be a nontrivial standard graph. Let f be an eigenfunction corresponding to an eigenvalue $k > \frac{\pi}{L_{\min}}$, where L_{\min} is the minimal edge length of Γ . Let Ω be a Neumann domain of f .*

- (1) If Ω contains a vertex $v \in \mathcal{V}$ of degree $d_v > 2$ then Ω is a *star graph* with $\deg(v)$ edges.
- (2) If Ω does not contain a vertex $v \in \mathcal{V}$ of degree $d_v > 2$ then Ω is a *path graph*, of length $\frac{\pi}{k}$.

Proof. For any edge $e \in \mathcal{E}$ we have that $f|_e(x) = B_e \cos(kx + \varphi_e)$, where B_e, φ_e are some edge dependent real parameters. This together with $k > \frac{\pi}{L_{\min}}$ implies that the derivative of f vanishes at least once at the interior of each edge. Hence, the set of Neumann points, $\mathcal{N}(f)$ contains at least one point on each edge. It follows that each Neumann domain contains at most one vertex of Γ . Thus, there are two types of Neumann domains: if a Neumann domain, Ω , contains a vertex with $\deg(v) > 2$ then Ω is a *star graph*, whose number of edges is d_v ; otherwise Ω is a *path graph*. A Neumann domain which is a path

graph can be parameterized as $\Omega = [0, l]$. Since $f'(0) = 0$ we get that $f|_{\Omega}(x) = \cos(kx)$ up to a multiplicative constant. Using $f'(l) = 0$ and that f' does not vanish in the interior of Ω we conclude $l = \frac{\pi}{k}$. \square

Remark. Only finitely many eigenvalues do not satisfy the condition $k > \frac{\pi}{L_{\min}}$ in the lemma. The number of those eigenvalues is bounded by

$$\left| \left\{ n \in \mathbb{N} : 0 \leq k_n \leq \frac{\pi}{L_{\min}} \right\} \right| \leq 2 \frac{|\Gamma|}{L_{\min}},$$

where $|\Gamma| = \sum_{e \in \mathcal{E}} L_e$ is the total sum of all edge lengths of Γ . This can be shown using

$$(8.1) \quad \forall n \in \mathbb{N}, \quad k_n \geq \frac{\pi}{2|\Gamma|} (n+1),$$

which is the statement of Theorem 1 in [31].

To complement the lemma above, we note that there are also Neumann domains which are not simply connected. Indeed, consider the graph Γ depicted in Figure 8.2(i). It has an eigenfunction with no Neumann points, so that the eigenfunction has a single Neumann domain which is the whole of Γ and in particular, it is not simply connected (Figure 8.2(ii)).

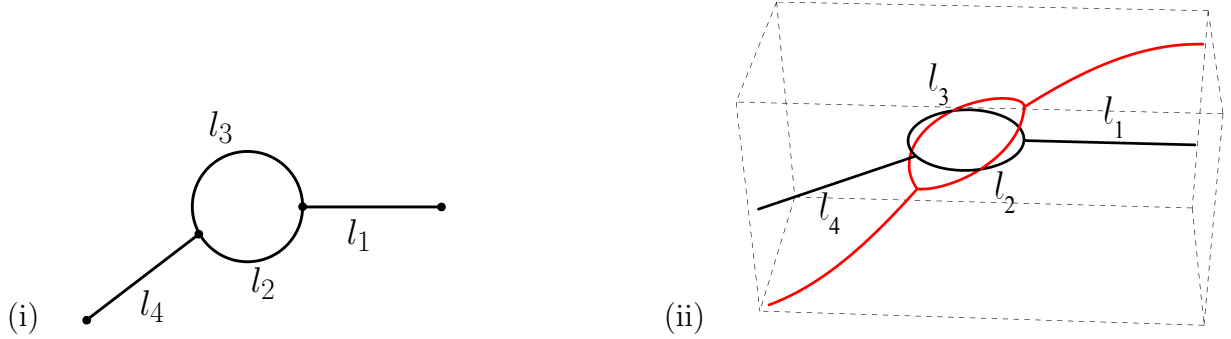


FIGURE 8.2. (i) A graph Γ with (ii) An eigenfunction whose single Neumann domain is not simply connected.

8.2. Critical points and nodal points - number and position. In the following we consider the critical points and nodal points of $f|_{\Omega}$. Note that, by definition, a Morse function on a one dimensional interval cannot have a saddle point. Hence, all critical points of a Morse eigenfunction of a graph are extremal points. We reuse the notations from the manifold part: $\mathcal{X}(f)$ for extremal points of f and $\mathcal{M}_+(f)$ ($\mathcal{M}_-(f)$) for maxima (minima). Denote by $\phi(f|_{\Omega})$ the number of nodal points of $f|_{\Omega}$, by E_{Ω} the number of edges of Ω , by V_{Ω} the number of its vertices, and by $\partial\Omega$ the vertices of Ω which are of degree one.

Proposition 8.3. [2] *Let f be a generic eigenfunction and Ω a Neumann domain of f . Then*

- (1) The extremal points of $f|_{\Omega}$, which are located on Ω are exactly the boundary of Ω , i.e., $\mathcal{X}(f) \cap \Omega = \partial\Omega$
- (2) $1 \leq |\mathcal{M}_+(f) \cap \partial\Omega| \leq |\partial\Omega| - 1$ (and the same bounds for $|\mathcal{M}_-(f) \cap \partial\Omega|$).
- (3) $1 \leq \phi(f|_{\Omega}) \leq E_{\Omega} - V_{\Omega} + |\partial\Omega|$.

Remark. Note that when Ω is a path graph the proposition implies that it has exactly one maximum, one minimum and one nodal point. Also, when Ω is a tree graph, the last part of the proposition gives $1 \leq \phi(f|_\Omega) \leq |\partial\Omega| - 1$.

9. GEOMETRY OF Ω

Similarly to the manifold case we use the normalized area to perimeter ratio to quantify the geometry of a Neumann domain. The following is to be compared with Definition 4.2.

Definition 9.1. Let f be a Morse eigenfunction corresponding to the eigenvalue k . Let Ω be a Neumann domain of f , whose edge lengths are $\{l_j\}_{j=1}^{E_\Omega}$. We define the normalized area to perimeter ratio of Ω to be

$$\rho(\Omega) := \frac{|\Omega|}{|\partial\Omega|} k,$$

where $|\Omega| = \sum_{j=1}^{E_\Omega} l_j$ and $|\partial\Omega|$ is the number of boundary vertices of Ω .

For graphs we are able to obtain global bounds on $\rho(\Omega)$.

Proposition 9.2. [2] *Let Ω be a Neumann domain. We have*

$$(9.1) \quad \frac{1}{|\partial\Omega|} \leq \frac{\rho(\Omega)}{\pi} \leq \frac{E_\Omega}{|\partial\Omega|}.$$

*If Ω is a star graph then we have a better upper bound $\frac{\rho(\Omega)}{\pi} \leq 1 - \frac{1}{|\partial\Omega|}$.
If Ω is a path graph then $\rho(\Omega) = \frac{\pi}{2}$.*

Next, we study the probability distribution of ρ . We find that for this purpose, it is useful to consider separately only the Neumann domains containing a particular vertex. Let Γ be a nontrivial standard graph and let f_n be its n^{th} eigenfunction. Assume that f_n is generic. Then, for any vertex $v \in \mathcal{V}$ there is a unique Neumann domain of f_n which contains v and we denote it by $\Omega_n^{(v)}$.

Proposition 9.3. [2] *Let $v \in \mathcal{V}$ of degree $d_v > 2$. The value of $\frac{1}{\pi}\rho$ on $\{\Omega_n^{(v)}\}_{n=1}^\infty$ is distributed according to*

$$(9.2) \quad \lim_{N \rightarrow \infty} \frac{\left| \left\{ n \leq N : f_n \text{ is generic and } \frac{1}{\pi}\rho\left(\Omega_n^{(v)}\right) \in (a, b) \right\} \right|}{|\{n \leq N : f_n \text{ is generic}\}|} = \int_a^b \zeta^{(v)}(x) dx,$$

where $\zeta^{(v)}$ is a probability distribution supported on $[\frac{1}{d_v}, 1 - \frac{1}{d_v}]$.

Furthermore, it is symmetric around $\frac{1}{2}$, i.e. $\zeta^{(v)}(x) = \zeta^{(v)}(1 - x)$.

Remark. If $d_v = 1$ then $\Omega_n^{(v)}$ is a path graph for all n , so that by Proposition 9.2 we get that $\zeta^{(v)}$ is a Dirac measure $\zeta^{(v)}(x) = \delta(x - \frac{1}{2})$.

As is implied by choice of notation, the distribution $\zeta^{(v)}$ indeed depends on the particular vertex $v \in \mathcal{V}$. We demonstrate this in Figure 9.1,(iii) where we compare between the probability distributions of two vertices of different degrees from the same graph. In addition, Figure 9.1,(vi) shows a comparison between the probability distributions of two vertices of the same degree from different graphs. The numerics suggest that the distributions are different, which implies that $\zeta^{(v)}$ may depend on the graph connectivity and not only on the degree of the vertex. It is of interest to further investigate this distribution, $\zeta^{(v)}$, and in particular its dependence on the graph's properties.

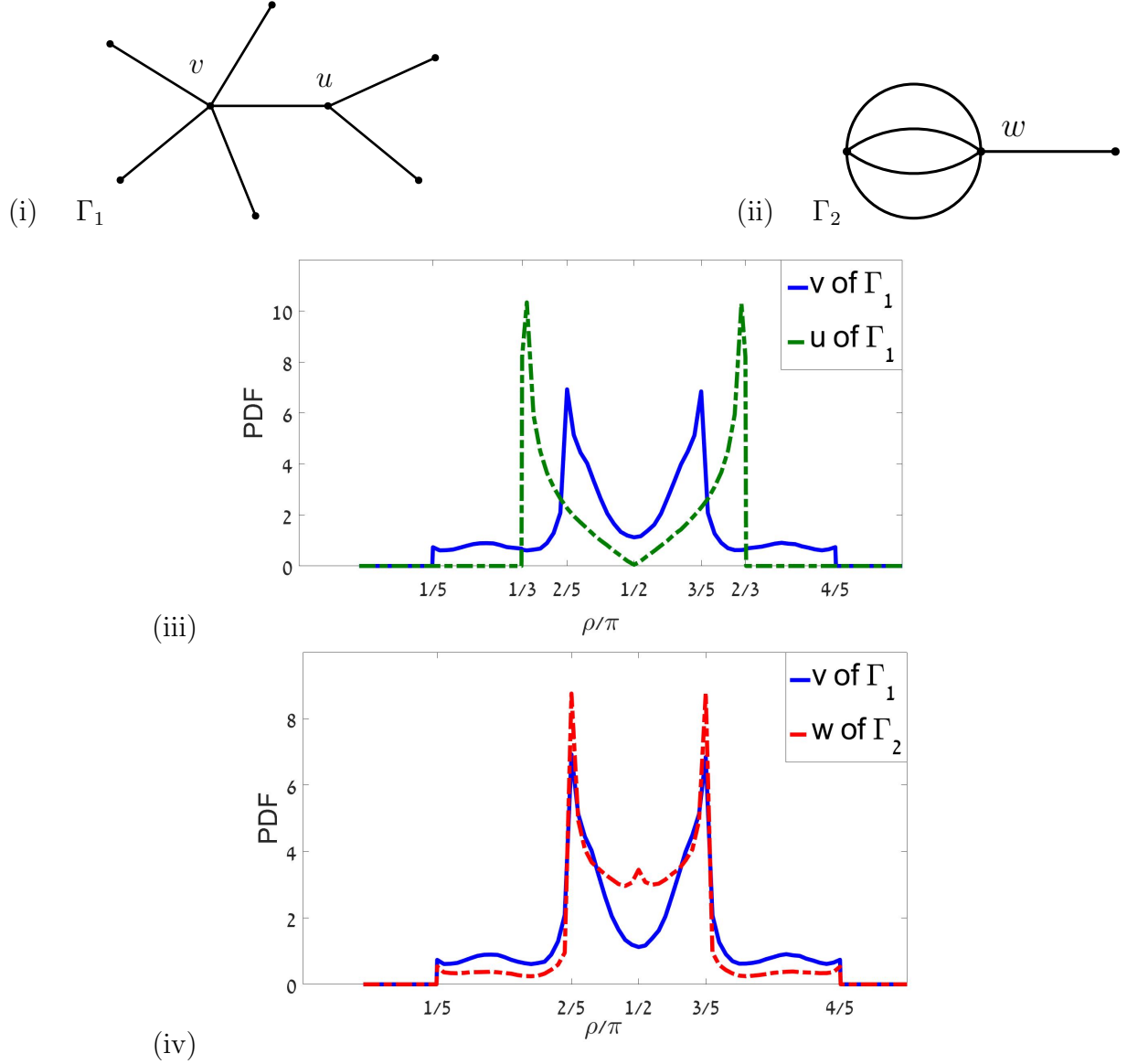


FIGURE 9.1. (i) Γ_1 , with vertices v , u of degrees 5, 3, correspondingly. (ii) Γ_2 , with vertex w of degree 5. (iii) A probability distribution function of $\frac{\rho}{\pi}$ -values for the Γ_1 Neumann domains which contain v (i.e., $\zeta^{(v)}$ in (9.2)) compared with $\zeta^{(u)}$. (iv) Similarly, $\zeta^{(v)}$ compared with $\zeta^{(w)}$.

All the numerical data was calculated for the first 10^6 eigenfunctions and for a choice of rationally independent lengths.

10. SPECTRAL POSITION OF Ω

By Lemma 8.1, a graph eigenvalue k appears in the spectrum of each of its Neumann domains. Exactly as in Definition 5.1 for manifolds, we define the spectral position of a Neumann domain Ω , as the position of k in the spectrum of Ω and denote it by $N_\Omega(k)$. Also, as in the manifold case, we have that $N_\Omega(k) \geq 1$ for graphs and for exactly the same reason (see discussion after Definition 5.1).

A useful tool in estimating the spectral position is the following lemma, connecting the spectral position of Ω to the nodal count of $f|_\Omega$.

Lemma 10.1. [2] *Let Γ be a nontrivial standard graph, f be a generic eigenfunction of Γ corresponding to an eigenvalue k and let Ω be a Neumann domain of f , which is a tree graph. Then*

$$(1) \ N_{\Omega}(k) = \phi(f|_{\Omega}).$$

$$(2) \ N_{\Omega}(k) \leq |\partial\Omega| - 1.$$

In particular if Ω is a path graph then $N_{\Omega}(k) = 1$.

The statement in (1) was proven in [12, 49, 53] under the assumption that $f|_{\Omega}$ is generic. This is indeed the case since f itself is generic and Ω is a tree graph (see remark after Lemma 8.1). The statement in (2) follows as a combination of (1) with Proposition 8.3,(3).

We further remark on the applicability of the lemma above; it applies for almost all Neumann domains. Indeed, for any given graph, all Neumann domains except finitely many are star graphs or path graphs (by Lemma 8.2), and those are particular cases of tree graphs.

Next, we show that the value of the spectral position implies bounds on the value of ρ , just as we had for manifolds (Proposition 5.2). For manifolds we got upper bounds on ρ , whereas for graphs we get bounds from both sides.

Proposition 10.2. [2] *Let Γ be a nontrivial standard graph, f be an eigenfunction of Γ corresponding to an eigenvalue k and let Ω be a Neumann domain of f . Then*

$$(10.1) \quad \frac{\rho(\Omega)}{\pi} \geq \frac{1}{|\partial\Omega|} \left(\frac{N_{\Omega}(k) + 1}{2} \right).$$

If Ω is a star graph then we further have the upper bound

$$(10.2) \quad \frac{\rho(\Omega)}{\pi} \leq \frac{1}{2} + \frac{1}{|\partial\Omega|} \left(\frac{N_{\Omega}(k) - 1}{2} \right).$$

Remark. Note that if $N_{\Omega}(\lambda) > 1$ then the bound in (10.1) improves the lower bound given in Proposition 9.2. Similarly, if Ω is a star graph and $N_{\Omega}(\lambda) < |\partial\Omega| - 1$, then the bound (10.2) improves the upper bound given in Proposition 9.2 for star graphs.

Next, we show that the spectral position has a well-defined probability distribution. As in the previous section (Proposition 9.2), we find that this distribution is best described when one focuses on Neumann domains containing a particular graph vertex.

Proposition 10.3. [2] *Let $v \in \mathcal{V}$ of degree d_v . We have that the spectral position probability,*

$$(10.3) \quad P(N_{\Omega(v)} = j) := \lim_{N \rightarrow \infty} \frac{\left| \left\{ n \leq N : f_n \text{ is generic and } N_{\Omega_n(v)}(k_n) = j \right\} \right|}{\left| \left\{ n \leq N : f_n \text{ is generic} \right\} \right|}$$

is well defined. If we further assume that $d_v > 2$ then

$$(1) \ P(N_{\Omega(v)} = j) \text{ is supported in the set } j \in \{1, \dots, d_v - 1\}.$$

$$(2) \ P(N_{\Omega(v)} = j) \text{ is symmetric around } \frac{d_v}{2}, \text{ i.e., } P(N_{\Omega(v)} = j) = P(N_{\Omega(v)} = d_v - j).$$

If $d_v = 1$ then $P(N_{\Omega(v)} = j) = \delta_{j,1}$.

By the proposition the support and the symmetry of the spectral position probability depend on the degree of the vertex. Yet, vertices of the same degree, but from different graphs may have different probability distributions as is demonstrated in Figure

10.1,(iii). In addition, we show in Figure 10.1,(vi) how the conditional probability distribution of $\rho(\Omega)$ depends on the value of the spectral position N_Ω (compare with the bounds (10.1),(10.2)).

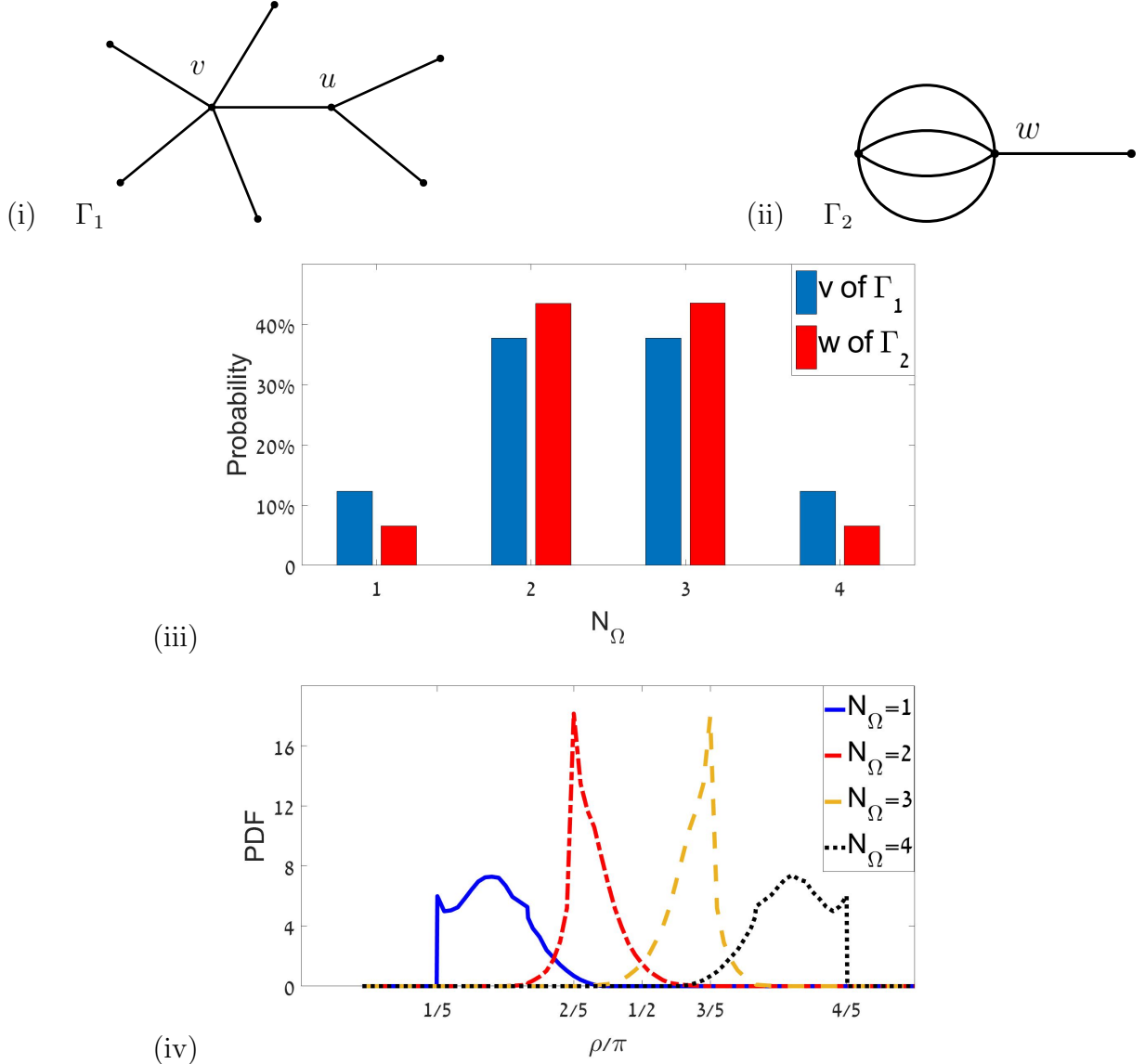


FIGURE 10.1. (i) Γ_1 , with vertex v of degree 5. (ii) Γ_2 , with vertex w of degree 5. (iii) The spectral position probability $P(N_{\Omega(v)} = j)$ for v of Γ_1 compared with $P(N_{\Omega(w)} = j)$ for w of Γ_2 . (iv) A probability distribution function of $\frac{\rho}{\pi}$ -values for the Γ_1 Neumann domains which contain v , conditioned on the value of the spectral position $N_{\Omega_n(v)}$.

All the numerical data was calculated for the first 10^6 eigenfunctions for a choice of rationally independent lengths.

11. NEUMANN COUNT

In this section we present bounds on the number of Neumann points and provide some properties of the probability distribution of this number.

Definition 11.1. Let Γ be a nontrivial standard graph and $\{f_n\}_{n=0}^\infty$ a complete set of its eigenfunctions. Denote by $\mu_n := \mu(f_n)$ and $\phi_n := \phi(f_n)$ the numbers of Neumann points and nodal points respectively. We call the sequences $\{\mu_n\}, \{\phi_n\}$ the Neumann count and nodal count, and the normalized quantities $\omega_n := \mu_n - n$, $\sigma_n := \phi_n - n$ are called the Neumann surplus and nodal surplus.

Proposition 11.2. [2] *Let Γ be a nontrivial standard graph. Let f_n be the n^{th} eigenfunction of Γ and assume it is generic. We have the following bounds:*

$$(11.1) \quad 1 - \beta \leq \sigma_n - \omega_n \leq \beta - 1 + |\partial\Gamma|,$$

and

$$(11.2) \quad 1 - \beta - |\partial\Gamma| \leq \omega_n \leq 2\beta - 1,$$

where $\beta = |\mathcal{E}| - |\mathcal{V}| + 1$ is the first Betti number of Γ .

Moreover, both quantities $\sigma_n - \omega_n$ and ω_n have well defined probability distributions, as stated in what follows.

Proposition 11.3. [2]

(1) *The difference between the Neumann and nodal surplus has a well defined probability distribution given by*

$$(11.3) \quad P(\sigma - \omega = j) = \lim_{N \rightarrow \infty} \frac{|\{n \leq N : f_n \text{ is generic and } \sigma_n - \omega_n = j\}|}{|\{n \leq N : f_n \text{ is generic}\}|}.$$

Furthermore, it is symmetric around $\frac{1}{2}|\partial\Gamma|$, i.e., $P(\sigma - \omega = j) = P(\sigma - \omega = |\partial\Gamma| - j)$.

(2) *The Neumann surplus has a well defined probability distribution which is symmetric around $\frac{1}{2}(\beta - |\partial\Gamma|)$.*

This proposition is in the spirit of the recently obtained result for the distribution of the nodal surplus [3]. It was shown in [3] that the nodal surplus, σ , has a well defined probability distribution which is symmetric around $\frac{1}{2}\beta$. The proof of Proposition 11.3 uses similar techniques to the proof of this latter result and appears in [2].

The proposition above also has an interesting meaning in terms of inverse problems. It is common to ask what one can deduce on a graph out of its nodal count sequence, $\{\phi_n\}$ [8, 9, 47]. It was found in [4] that the nodal count distinguishes tree graphs from others. The result already mentioned in [3] took a step further by showing that the nodal surplus distribution reveals the graph's first Betti number, as twice the expected value of the nodal surplus. However, it should be noted that all tree graphs have the same nodal count, so that one cannot distinguish between different trees in terms of the nodal count. Proposition 11.3 shows that the Neumann count, $\{\mu_n\}$ contains information on the size of the graph's boundary, $|\partial\Gamma|$. In particular, this enables the distinction between some tree graphs, which was not possible before.

Different tree graphs with the same boundary size, $|\partial\Gamma|$, have the same expected value for their Neumann count and are not distinguishable in this sense. Nevertheless, we may wonder whether the boundary size of a tree graph fully determines the probability distribution of its Neumann count. We do not have an answer to this question yet and carry on this exploration.

We end this section by noting that the bounds obtained in (11.2) on the Neumann surplus ω_n seem not to be strict, as we observed in many examples. Furthermore, we conjecture the following sharper bounds on ω_n .

Conjecture 11.4. *The Neumann surplus is bounded by*

$$-1 - |\partial\Gamma| \leq \omega_n \leq \beta + 1.$$

Proving the bounds (11.2) on ω_n is done by combining the bounds on $\sigma_n - \omega_n$ (11.1) with the bounds $0 \leq \sigma_n \leq \beta$ [17]. The bounds on both $\sigma_n - \omega_n$ and σ_n are known to be strict. Hence, if indeed the bounds on ω_n are not strict, it implies that the nodal surplus, σ_n , and the Neumann surplus, ω_n , are correlated when considered as random variables, which is an interesting result on its own.

Part 3. Summary

In this part we summarize the main results of this paper and focus on the comparison between analogous statements on graphs and manifolds. This is emphasized by using common terminology and notations for both graphs and manifolds.

Let f be an eigenfunction corresponding to the eigenvalue λ and Ω be a Neumann domain of f . On manifolds, we have that Ω and $f|_\Omega$ are of a rather simple form; Ω is simply connected; $f|_\Omega$ has only two nodal domains and its critical points are all located on $\partial\Omega$ (Theorem 3.2). On graphs, the situation is similar, as almost all Neumann domains are either star graphs or path graphs; it is possible to have other Neumann domains, and even non simply connected ones, only if λ is small enough (Lemma 8.2). For graphs, $f|_\Omega$ has two nodal domains if Ω is a path graph, but otherwise may have more, with a global bound on this number (Proposition 8.3,(3)).

The most basic property of Neumann domains is that $f|_\Omega$ is a Neumann eigenfunction of Ω (Manifolds - Lemma 3.1; Graphs - Lemma 8.1). The eigenvalue of $f|_\Omega$ is also λ and the interesting question is to find out what is the position of λ in the spectrum of Ω - a quantity which we denote by $N_\Omega(\lambda)$ (Definition 5.1). The intuitive feeling at the beginning of the Neumann domain study was that generically, $N_\Omega(\lambda) = 1$ or that at least the spectral position gets low values.

The general problem of determining the spectral position is quite hard for manifolds. The most general result we are able to provide for manifolds (Proposition 5.2) is a lower bound given in terms of the geometric quantity ρ , which is a normalized area to perimeter ratio (Definition 4.2). Interestingly, this result allows to estimate the spectral position numerically; a numerical calculation of ρ is rather easy compared to the involved calculation of the spectrum of an arbitrary domain, which is needed to determine a spectral position. This numerical method allows to refute the belief that for manifolds, generically, $N_\Omega(\lambda) = 1$. For graphs, the quantity ρ (Definition 9.1)) allows to bound the spectral position from both sides, for almost all Neumann domains (Proposition 10.2). Two additional results we have for the spectral position on graphs (but not for manifolds) are as follows. First, the spectral position of Ω is given explicitly by the nodal count of $f|_\Omega$, and this yields an upper bound on the spectral position (Lemma 10.1). Second, the spectral position has a limiting distribution which is symmetric (Proposition 10.3). Another point of comparison is that an upper bound on the spectral position, which we have for graphs, does not exist for manifolds. We show by means of an example that the spectral position

is unbounded in the manifold case. This example is given in terms of separable eigenfunctions on the torus. For this example, we show that although the spectral position of half of the Neumann domains is unbounded, it equals one for the other half (Theorem 5.3). This finding might imply that even though $N_\Omega(\lambda) = 1$ does not hold generically, there might be a substantial proportion of Neumann domains, for which it does hold (see e.g., (6.5)). This is indeed the case for graphs where the spectral position of each path graph Neumann domain equals one, and all of those form a substantial proportion of all Neumann domains (their number as well as their total length increase with the eigenvalue).

Finally, we discuss the Neumann domain count. On manifolds we count the number of Neumann domains, while on graphs we count the number of Neumann points. There is also a connection between the Neumann count and the nodal count. On manifolds, we have that the difference between the Neumann count and half the nodal count is non-negative (Corollary 6.1). On graphs, the difference between the Neumann count and the nodal count is bounded from both sides (Proposition 11.2). As for the Neumann count itself, it makes sense to consider it with a normalization: $\frac{\mu(f_n)}{n}$ on manifolds and $\mu(f_n) - n$ on graphs. For graphs we provide general bounds on $\omega_n = \mu(f_n) - n$ (Proposition 11.2), but believe that those are not sharp and conjecture sharper bounds (Conjecture 11.4). The validity of the conjecture would also imply a correlation between the nodal and the Neumann counts. In addition, ω_n possesses a limiting probability distribution which is symmetric (Proposition 11.3). The expected value of this distribution stores information on the size of the graph's boundary, $|\partial\Gamma|$; an information that is absent from the nodal count. Which other graph properties may be revealed by this distribution is still to be found. Turning back to manifolds, we treat separable eigenfunctions on the torus and for those derive the probability distribution of $\frac{\mu(f_n)}{n}$ (Proposition 6.4). This is to be viewed as the beginning of the analysis of Neumann count on manifolds. Two approaches in which some progress can be made are the following. One is getting a Courant-like bound of the form $\mu(f_n) \leq h(n)$, with h being possibly a linear function. The second would be studying the asymptotic behaviour, and for example showing that $\limsup_{n \rightarrow \infty} \mu(f_n) = \infty$. Both approaches are related to analogous results on nodal domains. The first is tied to the Courant bound for nodal domains (whose strict version does not hold for the Neumann count). The second is based on a series of works on asymptotic growth of the nodal count [32, 40, 41, 63] (see full description in Section 6) together with the basic bound (6.1) which relates the nodal count and the Neumann count.

ACKNOWLEDGMENTS

We thank Alexander Taylor for providing the python code [56] we used to generate the figures of Neumann domains on manifolds and calculate the distribution of ρ . The authors were supported by ISF (Grant No. 494/14).

APPENDIX A. BASIC MORSE THEORY

This section brings some basic statements in Morse theory which are useful for understanding the first part of the paper. For a more thorough exposition, we refer the reader to [10]. Throughout the appendix we take (M, g) be a compact smooth Riemannian manifold of a finite dimension. At some points of the appendix we specialize for the two-dimensional case and mention explicitly when we do so.

Definition A.1. Let $f : M \rightarrow \mathbb{R}$ be a smooth function.

- (1) f is a Morse function if at every critical point, $\mathbf{p} \in \mathcal{C}(f)$, the Hessian matrix, $\text{Hess}f|_{\mathbf{p}}$, is non-degenerate, i.e., it does not have any zero eigenvalues.
- (2) The Morse index $\lambda_{\mathbf{p}}$ of a critical point $\mathbf{p} \in \mathcal{C}(f)$ is the number of negative eigenvalues of the Hessian matrix, $\text{Hess}f|_{\mathbf{p}}$.

The following three propositions may be found in [10].

Proposition A.2. [10, Lemma 3.2 and Corollary 3.3]

If f is a Morse function then the critical points of f are isolated and f has only finitely many critical points.

Next, we consider the gradient flow $\varphi : \mathbb{R} \times M \rightarrow M$ defined by (2.2). For a particular $\mathbf{x} \in M$ we call the image of $\varphi : \mathbb{R} \times \mathbf{x} \rightarrow M$, a gradient flow line. Note that a gradient flow line, $\{\varphi(t; \mathbf{x})\}_{t=-\infty}^{\infty}$ has a natural direction dictated by the order of the t values.

Proposition A.3. [10, Propositions 3.18, 3.19]

- (1) *Any smooth real-valued function f decreases along its gradient flow lines. The decrease is strict at noncritical points.*
- (2) *Every gradient flow line of a Morse function f begins and ends at a critical point. Namely, for all $\mathbf{x} \in M$ both limits $\lim_{t \rightarrow \pm\infty} \varphi(t, \mathbf{x})$ exist and they are both critical points of f .*

Proposition A.4 (Stable/Unstable Manifold Theorem for a Morse Function). [10, Theorem 4.2]

Let f be a Morse function and $\mathbf{p} \in \mathcal{C}(f)$. Then the tangent space at \mathbf{p} splits as

$$T_{\mathbf{p}}M = T_{\mathbf{p}}^s M \oplus T_{\mathbf{p}}^u M,$$

where the Hessian is positive definite on $T_{\mathbf{p}}^s M$ and negative definite on $T_{\mathbf{p}}^u M$.

Moreover, the stable and unstable manifolds, (2.3), are surjective images of smooth embeddings

$$\begin{aligned} T_{\mathbf{p}}^s M &\rightarrow W^s(\mathbf{p}) \subseteq M \\ T_{\mathbf{p}}^u M &\rightarrow W^u(\mathbf{p}) \subseteq M. \end{aligned}$$

Therefore, $W^u(\mathbf{p})$ is a smoothly embedded open disk of dimension $\lambda_{\mathbf{p}}$ and $W^s(\mathbf{p})$ is a smoothly embedded open disk of dimension $m - \lambda_{\mathbf{p}}$, where m is the dimension of M .

Let us examine the implications of the results above in the particular case of Morse functions on a two-dimensional manifold.

- If \mathbf{q} is a maximum then $\lambda_{\mathbf{q}} = 2$ and so $W^u(\mathbf{q})$ is a two-dimensional open and simply connected set and $W^s(\mathbf{q}) = \{\mathbf{q}\}$.
- If \mathbf{p} is a minimum then $\lambda_{\mathbf{p}} = 0$ and so $W^s(\mathbf{p})$ is a two-dimensional open and simply connected set and $W^u(\mathbf{p}) = \{\mathbf{p}\}$.
- If \mathbf{r} is a saddle point then $\lambda_{\mathbf{r}} = 1$ and so both $W^s(\mathbf{r})$ and $W^u(\mathbf{r})$ are one-dimensional curves. Note that $W^s(\mathbf{r}) \cap W^u(\mathbf{r}) = \{\mathbf{r}\}$ and so we get that $W^s(\mathbf{r})$ is a union of two gradient flow lines (actually even Neumann lines) which end at \mathbf{r} . Similarly, $W^u(\mathbf{r})$ is a union of two gradient flow lines (Neumann lines) which start at \mathbf{r} .

By Definition 2.1 we get that Neumann domains are open two-dimensional sets and that the Neumann line set is a union of one dimensional curves. Moreover, those sets are complementary. Namely, the union of all Neumann domains together with the Neumann line

set gives the whole manifold [7, Proposition 1.3].

Next, we focus on a subset of the Morse functions, known as Morse-Smale functions, described by the following two definitions.

Definition A.5. We say that two sub-manifolds $M_1, M_2 \subset M$ intersect transversally and write $M_1 \pitchfork M_2$ if for every $\mathbf{x} \in M_1 \cap M_2$ the tangent space of M at \mathbf{x} equals the sum of tangent spaces of M_1 and M_2 at \mathbf{x} , i.e.

$$(A.1) \quad T_{\mathbf{x}}M = T_{\mathbf{x}}M_1 + T_{\mathbf{x}}M_2.$$

This is also called the *transversality condition*.

Definition A.6. A Morse function such that for all of its critical points $\mathbf{p}, \mathbf{q} \in \mathcal{C}(f)$ the stable and unstable sub-manifolds intersect transversely, i.e., $W^s(\mathbf{q}) \pitchfork W^u(\mathbf{p})$ is called a *Morse-Smale function*.

Let us assume now that M is a two-dimensional manifold and provide a necessary and sufficient condition for a Morse function to be a Morse-Smale function. First, for two critical points $\mathbf{p}, \mathbf{q} \in \mathcal{C}(f)$, the intersection $W^s(\mathbf{p}) \cap W^u(\mathbf{q})$ may be non-empty only for the following cases:

- (1) if $\mathbf{p} = \mathbf{q}$,
- (2) if \mathbf{p} is a minimum and \mathbf{q} is a maximum,
- (3) if \mathbf{p} is a minimum and \mathbf{q} is a saddle point,
- (4) if \mathbf{p} is a saddle point and \mathbf{q} is a maximum, or
- (5) if both \mathbf{p} and \mathbf{q} are saddle points.

In the first four cases, it is straightforward to check that the transversality condition is satisfied. In the last case we have that if $W^s(\mathbf{p}) \cap W^u(\mathbf{q}) \neq \emptyset$ then $W^s(\mathbf{p}) \cap W^u(\mathbf{q})$ equals to the gradient flow line (also Neumann line in this case) which asymptotically starts at \mathbf{q} and ends at \mathbf{p} . In such a case we get that for all $\mathbf{x} \in W^s(\mathbf{p}) \cap W^u(\mathbf{q})$, the tangent spaces obey $T_{\mathbf{x}}W^s(\mathbf{p}) = T_{\mathbf{x}}W^u(\mathbf{q})$ and those are one-dimensional, so their sum cannot be equal to the two-dimensional $T_{\mathbf{x}}M$. Therefore, in this case the transversality condition, (A.1) is not satisfied and as a conclusion we get

Proposition A.7. *On a two-dimensional manifold, a Morse function is Morse-Smale if and only if there is no Neumann line connecting two saddle points.*

By the Kupka-Smale theorem (see [10]) Morse-Smale gradient vector fields are generic among the set of all vector fields. Currently, there is no similar genericity result regarding eigenfunctions of elliptic operators which are Morse-Smale (in the spirit of [57, 58]). Our preliminary numerics suggest that Morse-Smale eigenfunctions are indeed generic.

REFERENCES

- [1] J. H. ALBERT, *Topology of the nodal and critical point sets for eigenfunctions of elliptic operators*, ProQuest LLC, Ann Arbor, MI, 1972. Thesis (Ph.D.)—Massachusetts Institute of Technology.
- [2] L. ALON AND R. BAND, *Neumann domains on quantum graphs*, In preparation.
- [3] L. ALON, R. BAND, AND G. BERKOLAIKO, *Nodal Statistics On Quantum Graphs*, Communications in Mathematical Physics, (2018).
- [4] R. BAND, *The nodal count $\{0, 1, 2, 3, \dots\}$ implies the graph is a tree*, Philos. Trans. R. Soc. Lond. A, 372 (2014), pp. 20120504, 24. preprint [arXiv:1212.6710](https://arxiv.org/abs/1212.6710).
- [5] R. BAND, G. BERKOLAIKO, H. RAZ, AND U. SMILANSKY, *The number of nodal domains on quantum graphs as a stability index of graph partitions*, Commun. Math. Phys., 311 (2012), pp. 815–838.

- [6] R. BAND, S. EGGER, AND A. TAYLOR, *Ground state property of Neumann domains on the torus*, ArXiv e-prints, (2017).
- [7] R. BAND AND D. FAJMAN, *Topological properties of Neumann domains*, Ann. Henri Poincaré, 17 (2016), pp. 2379–2407.
- [8] R. BAND, I. OREN, AND U. SMILANSKY, *Nodal domains on graphs—how to count them and why?*, in Analysis on graphs and its applications, vol. 77 of Proc. Sympos. Pure Math., Amer. Math. Soc., Providence, RI, 2008, pp. 5–27.
- [9] R. BAND, T. SHAPIRA, AND U. SMILANSKY, *Nodal domains on isospectral quantum graphs: the resolution of isospectrality?*, J. Phys. A, 39 (2006), pp. 13999–14014.
- [10] A. BANYAGA AND D. HURTUBISE, *Lectures on Morse Homology*, Kluwer Acad. Pub., 2004.
- [11] P. BÉRARD AND B. HELFFER, *The weak Pleijel theorem with geometric control*, J. Spectr. Theory, 6 (2016), pp. 717–733.
- [12] G. BERKOLAIKO, *A lower bound for nodal count on discrete and metric graphs*, Commun. Math. Phys., 278 (2007), pp. 803–819.
- [13] G. BERKOLAIKO, *Nodal count of graph eigenfunctions via magnetic perturbation*, Anal. PDE, 6 (2013), pp. 1213–1233. preprint [arXiv:1110.5373](#).
- [14] G. BERKOLAIKO AND P. KUCHMENT, *Introduction to Quantum Graphs*, vol. 186 of Mathematical Surveys and Monographs, AMS, 2013.
- [15] G. BERKOLAIKO, P. KUCHMENT, AND U. SMILANSKY, *Critical partitions and nodal deficiency of billiard eigenfunctions*, Geom. Funct. Anal., 22 (2012), pp. 1517–1540. preprint [arXiv:1107.3489](#).
- [16] G. BERKOLAIKO, H. RAZ, AND U. SMILANSKY, *Stability of nodal structures in graph eigenfunctions and its relation to the nodal domain count*, J. Phys. A, 45 (2012), p. 165203.
- [17] G. BERKOLAIKO AND T. WEYAND, *Stability of eigenvalues of quantum graphs with respect to magnetic perturbation and the nodal count of the eigenfunctions*, Philos. Trans. R. Soc. Lond. Ser. A Math. Phys. Eng. Sci., 372 (2014), pp. 20120522, 17.
- [18] S. BIASOTTI, L. DE FLORIANI, B. FALCIDIENO, P. FROSINI, D. GIORGI, C. LANDI, L. PAPALEO, AND M. SPAGNUOLO, *Describing shapes by geometrical-topological properties of real functions*, ACM Comput. Surv., 40 (2008), pp. 12:1–12:87.
- [19] G. BLUM, S. GNUTZMANN, AND U. SMILANSKY, *Nodal domains statistics: A criterion for quantum chaos*, Phys. Rev. Lett., 88 (2002), p. 114101.
- [20] V. BONNAILLIE-NOËL AND B. HELFFER, *Nodal and spectral minimal partitions—the state of the art in 2016*, in Shape optimization and spectral theory, De Gruyter Open, Warsaw, 2017, pp. 353–397.
- [21] J. BOURGAIN, *On Pleijel’s nodal domain theorem*, Int. Math. Res. Not. IMRN, (2015), pp. 1601–1612.
- [22] P. CHARRON, B. HELFFER, AND T. HOFFMANN-OSTENHOF, *Pleijel’s theorem for Schrödinger operators with radial potentials*, ArXiv e-prints, (2016).
- [23] A. CHATTOPADHYAY, G. VEGTER, AND C. K. YAP, *Certified computation of planar morse-smale complexes*, Journal of Symbolic Computation, 78 (2017), pp. 3 – 40. Algorithms and Software for Computational Topology.
- [24] Y. COLIN DE VERDIÈRE, *Magnetic interpretation of the nodal defect on graphs*, Anal. PDE, 6 (2013), pp. 1235–1242.
- [25] R. COURANT, *Ein allgemeiner Satz zur Theorie der Eigenfunktionen selbstadjungierter Differentialausdrücke*, Nachr. Ges. Wiss. Göttingen Math Phys, (1923), pp. 81–84.
- [26] S. DONG, P. BREMER, M. GARLAND, V. PASCUCI, AND J. C. HART, *Spectral surface quadrangulation*, in ACM SIGGRAPH 2006 Papers, SIGGRAPH ’06, New York, NY, USA, 2006, ACM, pp. 1057–1066.
- [27] H. EDELSBRUNNER, J. HARER, AND Z. A., *Hierarchical morse-smale complexes for piecewise linear 2-manifolds*, Discrete & Computational Geometry, 30 (2003), pp. 87–107.
- [28] H. EDELSBRUNNER, J. HARER, V. NATARAJAN, AND V. PASCUCI, *Morse-smale complexes for piecewise linear 3-manifolds*, in Proceedings of the nineteenth annual symposium on Computational geometry, SCG ’03, New York, NY, USA, 2003, ACM, pp. 361–370.
- [29] Y. ELON, S. GNUTZMANN, C. JOAS, AND U. SMILANSKY, *Geometric characterization of nodal domains: the area-to-perimeter ratio*, J. Phys. A: Math. Theor., 40 (2007), p. 2689.
- [30] H. FEDERER, *Geometric measure theory*, Die Grundlehren der mathematischen Wissenschaften, Band 153, Springer-Verlag New York Inc., New York, 1969.

- [31] L. FRIEDLANDER, *Extremal properties of eigenvalues for a metric graph*, Ann. Inst. Fourier (Grenoble), 55 (2005), pp. 199–211.
- [32] A. GHOSH, A. REZNIKOV, AND P. SARNAK, *Nodal domains of maass forms i*, Geometric and Functional Analysis, 23 (2013), pp. 1515–1568.
- [33] S. GNUTZMANN AND S. LOIS, *On the nodal count statistics for separable systems in any dimension*, J. Phys. A, 46 (2013), pp. 045201, 18.
- [34] S. GNUTZMANN AND U. SMILANSKY, *Quantum graphs: Applications to quantum chaos and universal spectral statistics*, Adv. Phys., 55 (2006), pp. 527–625.
- [35] P. V. GYULASSY A., BREMER P.-T., *Computing morse-smale complexes with accurate geometry*, IEEE Trans-actions on Visualization and Computer Graphics, 18 (2012).
- [36] B. HELFFER AND T. HOFFMANN-OSTENHOF, *On a magnetic characterization of spectral minimal partitions*, J. Eur. Math. Soc. (JEMS), 15 (2013), pp. 2081–2092.
- [37] B. HELFFER AND T. HOFFMANN-OSTENHOF, *A review on large k minimal spectral k -partitions and Pleijel’s theorem*, in Spectral theory and partial differential equations, vol. 640 of Contemp. Math., Amer. Math. Soc., Providence, RI, 2015, pp. 39–57.
- [38] B. HELFFER, T. HOFFMANN-OSTENHOF, AND S. TERRACINI, *Nodal domains and spectral minimal partitions*, Ann. Inst. H. Poincaré Anal. Non Linéaire, 26 (2009), pp. 101–138.
- [39] M. N. HUXLEY, *Area, Lattice Points, and Exponential Sums*, Clarendon Press, 1996.
- [40] J. JUNG AND S. ZELDITCH, *Number of nodal domains and singular points of eigenfunctions of negatively curved surfaces with an isometric involution*, J. Differential Geom., 102 (2016), pp. 37–66.
- [41] ———, *Number of nodal domains of eigenfunctions on non-positively curved surfaces with concave boundary*, Math. Ann., 364 (2016), pp. 813–840.
- [42] C. LÉNA, *Pleijel’s nodal domain theorem for Neumann and Robin eigenfunctions*, ArXiv e-prints, (2016).
- [43] P.-L. LIONS AND F. PACELLA, *Isoperimetric inequalities for convex cones*, Proc. Amer. Math. Soc., 109 (1990), pp. 477–485.
- [44] P.-L. LIONS, F. PACELLA, AND M. TRICARICO, *Best constants in Sobolev inequalities for functions vanishing on some part of the boundary and related questions*, Indiana Univ. Math. J., 37 (1988), pp. 301–324.
- [45] J. C. MAXWELL, *On hills and dales*, The London, Edinburgh, and Dublin Philosophical Magazine and Journal of Science, 40 (1870), pp. 421–427.
- [46] R. B. McDONALD AND S. A. FULLING, *Neumann nodal domains*, Philos. Trans. R. Soc. Lond. Ser. A Math. Phys. Eng. Sci., 372 (2014), pp. 20120505, 6.
- [47] I. OREN AND R. BAND, *Isospectral graphs with identical nodal counts*, J. Phys. A, 45 (2012), p. 135203. preprint [arXiv:1110.0158](https://arxiv.org/abs/1110.0158).
- [48] A. PLEIJEL, *Remarks on Courant’s nodal line theorem*, Communications on Pure and Applied Mathematics, 9 (1956), pp. 543–550.
- [49] Y. V. POKORNYĬ, V. L. PRYADIEV, AND A. AL’-OBEĬD, *On the oscillation of the spectrum of a boundary value problem on a graph*, Mat. Zametki, 60 (1996), pp. 468–470.
- [50] I. POLTEROVICH, *Pleijel’s nodal domain theorem for free membranes*, vol. 137 of Proc. Amer. Math. Soc., 2009.
- [51] M. REUTER, *Hierarchical shape segmentation and registration via topological features of laplace-beltrami eigenfunctions*, International Journal of Computer Vision, 89 (2010), pp. 287–308.
- [52] P. SARNAK AND I. WIGMAN, *Topologies of nodal sets of random band limited functions*, in Advances in the theory of automorphic forms and their L -functions, vol. 664 of Contemp. Math., Amer. Math. Soc., Providence, RI, 2016, pp. 351–365.
- [53] P. SCHAPOTSCHNIKOW, *Eigenvalue and nodal properties on quantum graph trees*, Waves in Random and Complex Media, 16 (2006), pp. 167–78.
- [54] S. STEINERBERGER, *A geometric uncertainty principle with an application to Pleijel’s estimate*, Ann. Henri Poincaré, 15 (2014), pp. 2299–2319.
- [55] G. SZEGÖ, *Inequalities for certain eigenvalues of a membrane of given area*, J. Rational Mech. Anal., 3 (1954), pp. 343–356.
- [56] A. J. TAYLOR, *pyneumann toolkit*. <https://github.com/inclement/neumann>, 2017.
- [57] K. UHLENBECK, *Eigenfunctions of Laplace operators*, Bull. Amer. Math. Soc., 78 (1972), pp. 1073–1076.

- [58] ———, *Generic properties of eigenfunctions*, Amer. J. Math., 98 (1976), pp. 1059–1078.
- [59] M. VAN DEN BERG, D. GRIESER, T. HOFFMANN-OSTENHOF, AND I. POLTEROVICH, *Geometric aspects of spectral theory*. Oberwolfach Report 33/2012, July 2012.
- [60] H. F. WEINBERGER, *An isoperimetric inequality for the N -dimensional free membrane problem*, J. Rational Mech. Anal., 5 (1956), pp. 633–636.
- [61] H. WEYL, *Über die asymptotische verteilung der eigenwerte*, Nachrichten von der Gesellschaft der Wissenschaften zu Göttingen, Mathematisch-Physikalische Klasse, 1911 (1911), pp. 110–117.
- [62] S. ZELDITCH, *Eigenfunctions and nodal sets*, Surveys in Differential Geometry, 18 (2013), pp. 237–308.
- [63] S. ZELDITCH, *Logarithmic lower bound on the number of nodal domains*, J. Spectr. Theory, 6 (2016), pp. 1047–1086.
- [64] A. ZOMORODIAN, *Topology for Computing*, Cambridge Monographs on Applied and Computational Mathematics, Cambridge University Press, 2005.

DEPARTMENT OF MATHEMATICS, TECHNION–ISRAEL INSTITUTE OF TECHNOLOGY, HAIFA
32000, ISRAEL